# New perspectives on intestinal morphogenesis: the role of cell division and intraepithelial forces in villus formation

**by**

**Andrew Michael Freddo**

**A dissertation submitted in partial fulfillment**
**of the requirements for the degree of**
**Doctor of Philosophy**
**(Cell and Developmental Biology)**
**in the University of Michigan**
**2016**

**Doctoral Committee:**

**Assistant Professor Jason Spence, Chair**
**Professor Deborah L. Gumucio**
**Professor Benjamin L. Margolis**
**Professor Kristen J. Verhey**
**Associate Professor Yukiko Yamashita**

This thesis is dedicated to Nana.
I think of you every single day.
You are greatly loved and missed.

# Acknowledgements

There is no way I could have made it to this point in my life without the support and guidance of so many people. Know that each and every one of you has shaped me into the man and scientist that I am today.

First and foremost, I would like to thank Dr. Deborah Gumucio for being a kind and supportive mentor. From my first days in the lab, when a simple antibody stain was a learning experience, to attempting to understand the complicated intersection of biology and physics we somehow ended up at, you have been there every step of the way. You have pushed me to look at problems from different perspectives and taught me how to defend my ideas. I have always felt like I could ask you for advice about anything, and I am looking forward to keeping in touch through the next stage of my training!

To the rest of the Gumucio Lab, my PhD would have been much less fruitful without your contributions, both scientific and otherwise. Kate, you were my first teacher about the villi, and I have been so fortunate to have you as a resource for scientific and life advice! Ken, know that whoever is stuck sitting next to your desk is very lucky. You've listened to my ramblings about my data and recipe planning, and it's been an honor to get to know you and your adorable family. Margaux, I could not have asked for a better undergraduate assistant to work with; your enthusiasm and sunny disposition gave me something to look forward to on even the darkest winter days. Michelle, thank you for being a mentor. As I'm continuing this dual degree journey,

it has been great to look up to someone on “the other side”. Deepa, we have shared many a laugh, maybe to the chagrin of those around us, and I have all the faith in your future success. Yue, you have brought a new perspective and fresh energy to the lab, and it has been great to have someone who’s better at math than me around! Sha, thanks for always lending a listening ear and being so supportive. Tracy, I’ll miss hearing about your upcoming travels and cat stories! Jierong, your devotion the lab has been second to none, thank you for helping me with all the mouse room work. To all the undergrads past and present, among them Ryan, Kyle, Nishita, and Juhi: juggling school and the lab is not easy, and it’s often too easy for us to forget. Lastly, to former lab members Neil, Shawn, Katherine, and Ajay: I’m so grateful for your guidance through the perils, trials, and tribulations of this PhD journey.

To my scientific collaborators, it has been an honor to learn from your different backgrounds. Santiago Schnell, Suzanne Shoffner, and Krishna Garikipati: you have all inspired me to think about biology from a new perspective, and though we’ve only known each other for a few months, you have truly helped me synthesize the last few years of data. To the Gut Group, especially the Samuelson lab, including current members Elise, Theresa, and Natacha, and former members Alexis and Gail: thank you for helping me through my attempts at Confetti, FlowJo, and of course the TC room. To the Wellik lab: Deneen, thank you for being a great first rotation mentor, Steve and Brian, thank you for teaching me all about the pancreas, how to handle mice, and putting up with my chemistry questions. To the Developmental Genetics Group: it was an honor to present to you, and your thought-provoking feedback helped me to really get closer to “the truth”.

To my thesis committee, current and former, Drs. Jason Spence, Ben Margolis, Kristen Verhey, Yukiko Yamashita, and Daniel Teitelbaum: I have looked forward to our meetings to get

to know you, feed you snacks, and share my scientific progress. Thank you for your input over the last few years.

I never would have had the opportunity to attend the University of Michigan if I had not had an amazing education at Caltech. To my first research mentor, Dr. Robert Grubbs: thank you for the unique and truly world-class research opportunity.

The beautiful images I've been fortunate enough to collect would not have been possible without the support I had from the MIL and Histology cores, Chris Edwards, Dotty Sorenson, Sasha Menshinchi, Judy Poore, and Jeff Harrison: you have been the most kind and supportive group, always able to answer even the most mundane of questions as I worked on million dollar machines! Shelley Almburg, I think about your kind words and positive presence every time I pass by the MIL.

None of this would have been possible without the administrative support of MSTP Office, Ron Koenig, Ellen Elkin, Hilkka Ketola, and Laurie Koivupalo: thank you so much for answering all of my e-mails and making me feel like I always had a home as I stood between medical and graduate schools. CDB, Kristen Hug, Lori Longeway, Brittney Longeway, Karen Lang, and Einor Jacobsen: we have the best staff, and I am so thankful for your patience in helping me figure out all of the logistical and reimbursement challenges I've encountered along the way!

To my friends, you made this road, dare I say, fun! Xixi, you literally were the first person I met here at Michigan and first (and last) person I would share my yogurt with. Natasha, I'm not going to let you forget that pancetta is not a cheese. Zach, I'll never forget our late-night chats at the retreat, and neither will our classmates. Alexis, I always looked up to you, and your

support, love, and delicious baking have taught me I can have it all – science and food. Caroline, my first "frenemy", I think we failed.

To my 2nd floor BSRB crew, Briana, Danielle, Alana, Kyriel, and Chris: it's been so fun to get to know you all over the water fountain. When I first came to the lab, I was unsure how I would fit in after saying goodbye to my med school classmates. However, you all made me feel immediately at home (with minimal food bribing), and I hope that we can keep in touch even when I'm back in the hospital!

I've also had the amazing opportunity to meet so many other groups during my six years here. The Saline group, Rainier, Roel, Karen, and Stefanie: thanks for including me in your Filipino parties! Those from the Med School Class of 2014: I'm so proud of all of you. I loved sharing our first two years of med school together. Especially of note are those "Gossip Girl" evenings, brunch dates (Hema, Sarah, Grace, Marci, Joe), hip hop dance sessions (Sarwar), and early morning swimming (Beth).

I truly can say I made life-long friends during my years at Caltech; although we no longer live near each other, I always look forward to meeting up or talking on the phone! Dannah, you are the one, the only Best Fr and I'm excited to be your Dr. Best Fr. Lisa and Mallika, we were quite the "terrible trio"! Caleb, I blame my scientific journey on you, and I'll never forget our first Chem Camp experience. Nadia, thank you for being so supportive of my scientific and personal growth over these formative years.

And of course, I must mention the friends I've known the longest. Brittany, Amy, Caryl, and the rest of the Science/Engineering class: I think those arduous days slaving over our senior projects prepared me for my current studies in some strange way. Tory, I'll never forget our 8th

grade antics. Joe, I'm still working on that Nobel Prize, but you're still on the invite list to Sweden!

Jose. My life would be incomplete without you. You deserve the most thanks for helping me through this four-year journey. Every single day, I can't believe how lucky I am to have found someone who makes me laugh, makes me think, and loves me unconditionally as you do. You understand my stress and are the calming influence I never knew I needed. None of the work in this thesis would have been possible without you. Thanks for breaking down your walls and opening your heart and your family to me.

Anyone who knows me even a little bit will tell you I am immensely proud of my heritage. Though I have not lived at home for the last decade, my heart is always with my family, both alive and deceased. I'll never forget the Sunday Dinners, card games, holidays, and trips to Vegas. All of these things are inextricably linked with who I am. I hope that what I have accomplished and will continue to accomplish will in some small way repay the sacrifices and unconditional love you have made and given to me. Even though I'm often absent, I think of you every single day.

To my parents, I have always known that I am the luckiest son in the world, and though I'm no longer your "sack of potatoes", I know that you are always there for me, no matter what is going on. I can't always explain what I do in the lab to you, but nonetheless you let me continue this academic journey; one day I'll get a "real job". Thank you for being so supportive and understanding when I happened to find myself along the way. I hope I can find a way to make my own family feel as loved as you continue to make me feel every day.

And lastly, I have been so extremely blessed in my life experiences and those I have met along the way. None of it would be possible without God, and the opportunity to study His creation, though frustrating at times, is ultimately such an honor.

# Table of Contents

# List of Figures

# List of Abbreviations

| | |
|---|---|
| AFM | Atomic force microscopy |
| AJ | Adherens junction |
| AMIS | Apical membrane initiation site |
| aPKC-PS | aPKC pseudosubstrate |
| Bmp | Bone morphogenetic protein |
| C-division | Crossing division |
| C-ERMAD | C-terminal ERM association domain |
| CDC42 | Cell division cycle 42 |
| CRB3 | Crumbs3 |
| DE | Definitive endoderm |
| DMSO | Dimethyl sulfoxide |
| EGF | Epidermal growth factor |
| ENS | Enteric nervous system |
| ERM | Ezrin-Radixin-Moesin protein family |
| EVL | Enveloping cell layer |
| EX.X | Embryonic day X.X |
| EZR | Ezrin |
| $Ez^{ShhKO}$ | $Ez^{flox/flox};Shh^{Cre\text{-}EGFP/+}$ mouse model |
| $Ez^{VillinKO}$ | $Ez^{flox/flox};Villin\text{-}Cre^{Tg/+}$ mouse model |

| | |
|---|---|
| F-actin | Filamentous actin |
| FERM | Band-four point one, Ezrin, Radixin, Moesin |
| FOXA2 | Forkhead box A2 |
| G2 phase | Gap 2 phase |
| hESC | Human embryonic stem cells |
| Hh | Hedgehog |
| IHH | Indian hedgehog |
| IKNM | Interkinetic nuclear migration |
| iPSC | Induced pluripotent stem cells |
| LGN | G-protein signaling modulator 2 |
| LKB1 | Serine/threonine kinase 11 |
| M phase | Mitosis |
| MDCK | Madin-Darby canine kidney |
| MVID | Microvillus inclusion disease |
| NF2 | Neurofibromin 2 (Merlin) |
| NUMA1 | Nuclear mitotic apparatus protein 1 |
| PAR | Partitioning defective |
| PDGF | Platelet-derived growth factor |
| pHH3 | Phospho-histone H3 |
| $PIP_2$ | Phosphatidylinositol 4,5-bisphosphate |
| PRKCZ | Protein kinase C zeta isoform (aPKC) |
| PTEN | Phosphatase and tensin homolog |
| PX | Postnatal day X |

| | |
|---|---|
| RAC1 | Ras-related C3 botulinum toxin substrate 1 |
| RHOA | Ras homolog family member A |
| ROCK | Rho-associated, coiled-coil containing protein kinase |
| SAG | Smoothened agonist |
| SCRIB | Scribbled planar cell polarity protein |
| SEM | Scanning electron microscopy |
| SHH | Sonic hedgehog |
| TGFβ | Transforming growth factor β |
| TEM | Transmission electron microscopy |
| TJ | Tight junction |
| VE | Visceral endoderm |
| VEGFA | Vascular endothelial growth factor A |
| ZO1 | Zona occludens 1 |

# Abstract

Finger-like projections called villi convolute the intestinal surface, maximizing the area for nutrient absorption. Villi are rapidly formed and patterned during embryonic development; in the mouse, beginning at embryonic day (E)14.5, one new villus is defined approximately every 15 minutes. In this thesis, we worked at the interface of advanced *in vivo* imaging and *in silico* mechanical modeling to understand the transformation from a flat intestinal surface into a field of domed villi.

For decades, villus morphogenesis was thought to involve formation of isolated lumens in a stratified epithelium. However, recent studies have shown that the pre-villus epithelium is a single pseudostratified layer and its surface remains connected throughout development. Here, we develop a new model that offers insight into how this dramatic lumenal surface expansion occurs within these parameters.

We determined that initial villus demarcation occurs by patterned invaginations in the intestinal surface. Their location is controlled by mesenchymal clusters, patterned structures that signal to cause the adjacent epithelium to shorten and widen. This shape change compresses the intervening epithelium. Within these regions, cell division-associated invaginations occur. These *in vivo* observations informed an *in silico* mechanical model of the epithelium, which

demonstrates that both compressive forces and cellular changes during mitosis can drive villus demarcation.

We also utilized the *Ezrin* null mouse model to define other cell behavior essential for villus morphogenesis; this model exhibits both ectopic lumens and villus fusions. We show that loss of EZRIN impairs mitotic spindle orientation control and transforms the epithelium into a stratified structure. In this context, ectopic lumens form between cell layers. Additionally, we establish that *Ezrin* plays a critical role in maintenance of the intestinal epithelium throughout life, and provide functional evidence of impaired junctional remodeling in the absence of EZRIN. Finally, we offer a unified model of how fused villi develop embryonically and postnatally.

Working at the interface between *in vivo* observations and *in silico* modeling will inform future studies on the biological and physical characteristics required for the dramatic epithelial convolution associated with villus development, potentially providing new avenues for the targeted engineering of intestinal surface.

# Chapter I

# Introduction*

The main function of the small intestine is to digest and absorb nutrients, many of which cannot be synthesized by cells and can only be obtained from the diet. For example, out of the twenty amino acids, nine are essential; if these are not derived from the diet, severe nutritional deficiencies can result (Trumbo et al., 2002). For maximally efficient absorption, the intestine has a large surface area (approximately 30 square meters), allowing for optimal contact between lumenal contents and the absorptive surface. Multiple morphological adaptations contribute to this large surface (Figure I-1), including the remarkable length of the intestine (from 2-4 meters) (Helander and Fändriks, 2014), convolution of its mucosa into finger-like projections known as villi (Mathan et al., 1976; Moxey and Trier, 1979), and the presence of microvilli on the apical surface of each absorptive epithelial cell, which constitute the intestinal brush border (Sauvanet et al., 2015). Villi and microvilli amplify the total intestinal surface area by about 6.5 and 13 times, respectively, and thus represent critical elements of surface expansion (Helander and Fändriks, 2014).

* Note this chapter is an expansion of the following review article

**Walton KD, Freddo AM, Wang S, and Gumucio DL.** (2016). Generation of intestinal surface: an absorbing tale. *Development*, invited review, Submitted.

If intestinal surface area is severely compromised, intestinal failure may result, a condition defined as inability to absorb sufficient nutrients to sustain life. One cause of intestinal failure is an extremely shortened intestine, which may occur due to a genetic disorder or a traumatic event. Unfortunately, limited treatment options exist for these patients, and they are often confined to life-long parenteral nutrition, or less commonly, may undergo intestinal transplantation (Goulet and Ruemmele, 2006; Goulet et al., 2004; Stelzner and Chen, 2006). Even in a setting of sufficient bowel length, clinical malnutrition can result from loss of intestinal villi. In patients with celiac disease, villus atrophy compromises surface area to prevent proper absorption (Walker-Smith et al., 1990). This emphasizes the essential role played by villi in increasing apical surface. Lastly, absorptive surface area may be compromised by incorrect formation of microvilli. In patients with microvillus inclusion disease (MVID), the normally well-organized arrangement of microvilli at the apical surface is disrupted. Instead, vesicular "inclusions" containing internal microvilli are seen within absorptive epithelial cells. This can manifest as early as the first days of life, and carries a high mortality (Ruemmele et al., 2010). MVID is associated with a wide variety of genetically inherited mutations, many of which involve proteins involved in apical vesicular trafficking (Ruemmele et al., 2010; Wiegerinck et al., 2014).

Although all of these adaptations for increasing intestinal surface area (lengthening, formation of villi, and elaboration of microvilli) are important for proper health, this thesis will focus on the epithelial changes that occur during formation of the initial intestinal villi. Despite their importance to surface area amplification, little is currently known about how they form in the fetus. Evidence from animal and clinical models of bowel resection suggests this is the critical time for maximum villus development. In rodent models of intestinal resection, although

the intestine may adapt by altering length and villus structure (increased height and girth), new villi do not appear to form efficiently (Clarke, 1967; Forrester, 1972; Helmrath et al., 1996). In humans, adaptations in villus shape are also observed after bowel resection. However, data on new villus growth in the human are limited because clinical trials testing the effects of adaptation are difficult to conduct (Weale et al., 2005). Thus, to learn how the apical surface is expanded during villus formation, we concentrate here on the period of initial villus emergence during fetal life. Eventually, insights from these studies might provide clues as to how to stimulate growth of new villi in patients with intestinal failure or compromised intestinal surface area.

## Intestinal Morphogenesis and Differentiation

### *Gastrulation and endoderm specification*

The intestinal epithelium is polarized, with its internal apical surface facing an open lumen and its basal surface surrounded by mesenchyme. The epithelium is derived from the endoderm, which contains components derived from both definitive and visceral endoderm (Franklin et al., 2008; Kwon et al., 2008). Definitive endoderm is specified during gastrulation. During this process, cells in the anterior end of the primitive streak undergo an epithelial to mesenchymal transition by losing their initial apical-basal polarity and downregulating E-cadherin to allow them to migrate along the wings of the expanding mesoderm (Burtscher and Lickert, 2009; Viotti et al., 2014). As a result of unknown signals, some of these migrating cells intercalate into the visceral endoderm layer by undergoing a mesenchymal to epithelial transition. At this point, they establish their final polarity, with the apical surface on the interior of the embryo, and increase expression of junctional proteins to seal the epithelium (Figure I-2) (Nowotschin and Hadjantonakis, 2010; Viotti et al., 2014). FOXA2, a forkhead family

transcription factor, helps recruit the necessary signaling molecules for these processes. In mouse embryos, *Foxa2* mutations prevent apical-basal polarity and tight junction re-formation upon cellular integration into the developing endoderm (Burtscher and Lickert, 2009).

*Intestinal specification and villus patterning*

After gastrulation, the endoderm is a flat (in human) or cup-shaped (in mouse) epithelial sheet. In the mouse, this sheet is folded into a tubular structure between embryonic day (E)8.0 to E9.5 (Lewis and Tam, 2006). Even while folding occurs, the tube is being regionally specified by numerous cell signaling events into a series of organs, which make up the gastrointestinal tract (esophagus, stomach, small intestine, and colon) and accessory organs (lungs, thymus, thyroid, parathyroid, liver, and pancreas) (Spence et al., 2011).

The small intestine arises from the distal region of the foregut and the midgut. This region of the tube elongates between E10.5, when the first hairpin loop of the intestine is seen, and E14.5, and when villus morphogenesis initiates. During this time, the lumenal surface of the small intestinal tube is flat, but beginning at E14.5, the lumenal surface dramatically convolutes to form the first villi (Figure I-3). The pattern of villus location is mediated by bidirectional signaling between the epithelium and underlying mesenchyme. First, Hedgehog (Hh) ligand secreted from the epithelium signals to the underlying mesenchyme (Kolterud et al., 2009) to cause aggregation of mesenchymal cells into clusters. These clusters are tightly associated with the basement membrane and pattern where the villi will develop, such that one cluster corresponds to one villus domain. Clusters begin to form in the proximal intestine at E14.0 and spread in a wave-like pattern towards the distal intestine by E15.5 (Moxey and Trier, 1979; Walton et al., 2012).

Signaling pathways affect both the size and distribution of clusters, as highlighted by experiments using both *ex vivo* intestinal explant cultures and genetic modifications (Walton et al., 2012; Walton et al., 2016). Amazingly, explant cultures from intestines harvested before cluster formation will continue to grow and develop in culture for more than three days, though they grow slower than *in utero*. Small molecule agonists or inhibitors can be added to such cultures to observe the effect of signaling pathways on cluster and villus formation. For example, cyclopamine (which blocks Hh signaling) inhibits formation of clusters (and villi), while the Smoothened agonist (SAG, which increases Hh signaling) dramatically increases the cluster (and villus) size (Walton et al., 2012). Additionally, Bmp signaling controls the spacing of these clusters via a self-organizing field provided by a Turing-like activator/inhibitor system. Inhibition of Bmp either through small molecule treatment (with Dorsomorphin) or receptor knockout in clusters results in enlarged clusters and villi. This occurs independently of Bmp signaling to the overlying epithelium (Walton et al., 2016).

After initial villus specification, the intestine continues to grow both in length and girth, as additional rounds of villus formation occur. These new villi are patterned by new mesenchymal clusters, which form in the intervillus regions between established villi. In the mouse, a total of four rounds of villus formation occurs (Walton et al., 2012).

*Villus patterning occurs differently in the chick intestine*

Unlike the mouse small intestine, which transforms directly from a flat to a villus epithelium, the chick intestinal epithelium undergoes visible intermediate stages before villi are defined. The chick intestinal surface first convolutes into ridges, then zig-zags, and finally villi (Burgess, 1975). These stepwise changes correlate with consecutive formation of smooth muscle

layers surrounding the epithelial tube. Relieving the physical compression caused by these muscles reduces the convolution of the epithelial surface (Shyer et al., 2013).

Interestingly, while the same signaling molecules (Hh and Bmp) are involved in villus formation and patterning in the mouse and chick, the mechanisms by which these signals act are different. In the chick, the epithelial deformation caused by muscle formation described above creates localized maxima of Hh ligands, which in turn locally activates mesenchymal cluster genes, including *Bmp4*. *Bmp4* then acts on overlying epithelium to inhibit epithelial cell proliferation directly over the clusters; proliferation continues in the inter-cluster regions, promoting villus outgrowth (Shyer et al., 2015). In contrast, in the mouse, muscle development does not correlate with villus development. Thus, in the murine system, tensile forces do not pattern the field of villi, though confinement provided by the already developed inner circular muscle might play a role in aiding villus outgrowth (Walton et al., 2016; Walton et al., 2012). Also in the mouse, Bmp signals do not restrict epithelial proliferation over the clusters as in the chick; in fact, inhibition of Bmp signal reception by the epithelium does not alter villus patterning or epithelial proliferation (Walton et al., 2016). As described above, villus patterning in the mouse model seems to be independent of muscle development and instead dependent upon a Turing-like field patterning mechanism (Walton et al., 2016). Clusters themselves are signaling centers that express a variety of soluble signals that not only affect their distribution, but also likely promote changes in epithelial cell shape and proliferation to aid in villus outgrowth (Karlsson et al., 2000; Walton et al., 2016).

*Understanding epithelial changes that initiate villus morphogenesis*

The early epithelium (E12.0-E14.0) contains tightly packed cells with staggered nuclei, features that led early researchers to believe that the epithelium was stratified (Mathan et al., 1976). However, recent work has shown that this early epithelium is actually pseudostratified. Cell shape tracing shows that all cells contact both the apical and basal surfaces (Figure I-4D). Instead of arising due to multiple cell layers, the staggered appearance of nuclei is related to the process of interkinetic nuclear migration (IKNM) (Figure I-4A-C) (Grosse et al., 2011), in which nuclear position changes throughout the cell cycle such that nuclei are in constant movement in the apical-basal direction. M phase (mitosis) occurs at the apical surface and S phase (DNA replication) occurs at the basal surface (Lee and Norden, 2013; Meyer et al., 2011).

The early, flat epithelium is also relatively homogenous with respect to expression of critical signaling ligands, such as Sonic hedgehog (SHH), Indian hedgehog (IHH), and PDGFA (Karlsson et al., 2000; Kolterud et al., 2009). Additionally, nearly all cells in this quickly expanding pseudostratified epithelium appear to be proliferating (Grosse et al., 2011). At E14.5-E15.5, as the first villi are emerging in a wave down the tube, this pattern dramatically changes. Expression of SHH and PDGFA becomes rapidly restricted to intervillus regions, while IHH remains expressed throughout the villus and intervillus regions (Karlsson et al., 2000; Kolterud et al., 2009). *In situ* hybridization studies show that expression of *Axin2* is also restricted to the intervillus epithelial cells after villi form (Li et al., 2009). AXIN2 is a sensitive readout of Wnt signaling, a pathway that is not active in the intestinal epithelium at E14.5 (Li et al., 2009) and appears to only be strongly activated after this time (Dr. Jason Spence, unpublished). Thus, villus emergence is accompanied by activation of Wnt signaling at the base of the growing villi. Proliferation is also progressively restricted to intervillus regions as cells on the extending villi

withdraw from the cell cycle. As villi grow, the epithelial cell shape changes from a pseudostratified to a simple columnar epithelium, first on the villi and later in the intervillus regions (Figure I-4E-F) (Grosse et al., 2011).

Because the ultimate function of the villi is to amplify surface area so as to promote efficient absorption of nutrients across the apical surface of enterocytes, it is important to think of these morphogenic events in terms of apical surface expansion; the apical surface area expands three to four fold as it transforms from a flat to its initial villus structure. When it was thought that the early epithelium was stratified, lumen expansion was believed to occur due to *de novo* formation of secondary lumens within the stratified epithelium, which then coalesced with the main lumen to "carve" out the villi (Mathan et al., 1976). Further evidence for this mechanism came from a mouse model in which *Ezrin*, a gene that encodes an apical surface protein, was mutated. The resulting fused villi and ectopic lumens were thought to be the result of failure of these secondary lumens to merge with the main lumen and properly carve out villi (Saotome et al., 2004).

However, in light of recent data, the conclusions made on the basis of this phenotype must be re-examined. First, the intestinal epithelium is pseudostratified, not stratified. Second, secondary lumens do not form during normal villus development. Rather, all apical surfaces are continuous during this time (Grosse et al., 2011). Because intestinal apical surface expansion is such an essential process for growth and homeostasis, the work in my thesis is dedicated to investigating the cellular and molecular mechanisms underlying this process. In fact, villi form the structural platform for the generation of the microvillus brush border, which forms the mature apical surface of intestinal absorptive cells. Factors that compromise the formation or maintenance of villi will also lead to loss of the microvilli. Though the work in this thesis relates

to apical surface generation during villus formation, the following section provides a brief overview of the maturation of this apical surface to form microvilli.

*Microvillus formation further expands apical surface*

Microvilli are specialized cellular projections with cores composed of crosslinked actin bundles (about 20 polarized filaments per microvillus) that convolute the apical membrane of each epithelial cell (Figure I-5). Similar structures are found in some other polarized epithelia, such as the proximal tubules of the kidney (Fath and Burgess, 1995; Sauvanet et al., 2015).

Three main actin-binding proteins are important for forming and stabilizing microvilli: villin, fimbrin, and espin. Villin is initially expressed in the gut epithelium beginning at E10.0 and becomes apically concentrated at E13.5 (Ezzell et al., 1989). Although villin is important for the first phase of microvillus formation, in which actin filaments nucleate at electron-dense plaques in the apical actin terminal web (Fath and Burgess, 1995; Sauvanet et al., 2015), transfection of villin is not sufficient to generate microvilli *in vitro* (Fath and Burgess, 1995). Fimbrin, another actin cross-linker, is not expressed until E16.5, after villus formation has occurred (Ezzell et al., 1989). It binds to a different domain of F-actin than villin (Hampton et al., 2008; Sauvanet et al., 2015) and increases microvillus stiffness and order (Ezzell et al., 1989; Fath and Burgess, 1995). Unlike villin and fimbrin, espin attaches to F-actin monomers. It is recruited after the microvilli have been formed and stabilized by villin and fimbrin (Bartles et al., 1998; Loomis et al., 2006; Loomis et al., 2003).

Each of these proteins has been mutated individually and in combination, with only minimal effects on overall microvillus structure and function (Ferrary, 1999; Grimm-Gunter et al., 2009; Pinson et al., 1998; Zheng et al., 2000). In fact, mutating all three of these proteins

results in a similar effect to loss of fimbrin alone (short microvilli with disorganized cores). Because microvilli still form in these mice, compensation by other, unknown molecules is likely (Revenu et al., 2012).

A few apical proteins (further discussed in the following section) also are important for microvillus stability. For example, mutation of Ezrin (EZR), which crosslinks actin to the apical membrane, shortens microvilli in addition to perturbing villus architecture as noted above (Saotome et al., 2004). Similarly, loss of Crumbs3 (CRB3), another apical protein that binds Ezrin and participates in tight junction formation, shortens microvilli, similar to the Ezrin knockout (Whiteman et al., 2014).

## Cell Polarity

*Functional importance of cell polarity in epithelia*

The work in this thesis involves investigation of apical surface expansion, a process that is intimately connected to molecular polarization of cell surfaces. All epithelia have an apical and a basal surface, with junctional zones separating these domains and sealing epithelial cells together. These surfaces are marked by unique sets of proteins intended to perform distinct functions (Karner et al., 2006). In the intestine, the apical surface is highly specialized for nutrient digestion and absorption, and junctional integrity is essential for preventing pathogens from crossing into the body (Andrew and Ewald, 2010).

Epithelia are classified based on both cell shape and number of cell layers. Squamous epithelial cells have short lateral surfaces and wide apical surfaces, cuboidal cells have similarly sized apical and lateral domains, and columnar cells have a large lateral and shorter apical surface. Epithelia may consist of one cell layer (“simple” epithelium), multiple cell layers

("stratified"), or one cell layer with staggered nuclei, giving the appearance of multiple layers ("pseudostratified") (Figure I-6)(Karner et al., 2006; Rodriguez-Boulan and Macara, 2014). As noted above, during its development, the small intestinal epithelium changes from a pseudostratified epithelium to a simple columnar epithelium (Grosse et al., 2011).

Epithelial cells are also polarized with respect to their organelle distribution. In simple epithelia, nuclei are located basally, with the Golgi and endosomes closer to the apical surface. This allows for directed trafficking of proteins to or from the apical surface (Rodriguez-Boulan and Macara, 2014).

*Molecular determinants of polarity*

The apical and basolateral domains of epithelial cells are defined by a stereotyped pattern of proteins and phospholipids (Figure I-7). Four major classes of proteins establish and maintain polarity, including: PAR (partitioning) proteins, CRB (Crumbs), SCRIB (Scribbled), and the Rho GTPases. The six *Par* genes were discovered in *Caenorhabditis elegans* after a genetic screen for polarity disruptors (Kemphues et al., 1988); five of these have mammalian homologues (Rodriguez-Boulan and Macara, 2014). Each of these proteins has a specific sub-cellular localization: PAR-1 is basolaterally localized, PAR-3 is at the junctional complex, PAR-5 is diffusely cytoplasmic, and PAR-6 is in an apical complex (Karner et al., 2006; Rodriguez-Boulan and Macara, 2014). CRB is a transmembrane apical surface protein; its extracellular domain promotes correct apical membrane establishment and its intracellular domain interacts with other apical determinants (Tepass, 2012). SCRIB is found at the basolateral surface adjacent to the junctional complex (Nelson, 2003). Of the Rho GTPase class of polarity proteins, the most well studied members are CDC42, RAC1, and RHOA. These proteins integrate the actin

cytoskeleton with the polarity program and help to control intracellular vesicular trafficking (Rodriguez-Boulan and Macara, 2014). CDC42, originally discovered in budding yeast, is important for defining the apical zone (Karner et al., 2006; Qin et al., 2010; Rodriguez-Boulan and Macara, 2014). RAC1 organizes the cortical actin cytoskeleton, and RHOA effects contractile forces through regulation of actinomyosin filament assembly (Rodriguez-Boulan and Macara, 2014), thereby controlling cell shape.

The Ezrin-Radixin-Moesin (ERM) proteins also are apically localized. Although they are expressed in different tissues, ranging from various epithelia (Ezrin) to hepatocytes (Radixin) to endothelium (Moesin), all of these proteins link the actin cytoskeleton (via the C-ERMAD domain) to the apical plasma membrane either directly via $PIP_2$ binding or via ERM-binding proteins interacting with the FERM domain (Berryman et al., 1993; Fehon et al., 2010). ERM activation occurs by phosphorylation of the T567 residue (on Ezrin, T564 on Radixin, T558 on Moesin) by Rho kinase or protein kinase C zeta isoform (aPKC, PRKCZ) (Bretscher et al., 2002; Liu et al., 2013). Further modulation of ERM activity occurs through $PIP_2$ interacting with other resides (Braunger et al., 2014; Jayasundar et al., 2012). In addition to their role in apical polarity, ERM proteins modulate membrane tension based on the number of attachments to the apical surface (Braunger et al., 2014; Brückner et al., 2015).

Junctional complexes both seal epithelial cells together and separate apical and basal domains. In vertebrates, the two main types of junctions are tight (TJ) and adherens junctions (AJ) (Nelson, 2003). The TJ are anchored by the transmembrane Occludin and Claudin proteins, which interact via their cytoplasmic tails with the Zona Occludens (ZO) proteins (ZO1, 2, 3) (Fleming et al., 2000). The AJ are more basally localized than the TJ, anchored by transmembrane Cadherins (such as E-cadherin), and connected to p120, β-catenin, and α-catenin

(Nelson, 2003; Takeichi, 2014). The AJ also connect to the actin cytoskeleton; this controls cell shape in coordination with the activity of Rho GTPases and their targets, such as ROCK. Such contractile events can result in apical constriction, an important step in changing tissue shape (Takeichi, 2014).

*Creation and maintenance of cell polarity*

Creating and maintaining cell polarity is a highly complex process, which differs slightly among different organisms and even among epithelia within the same organism. However, some conserved mechanisms have been identified and these are important in the context of lumen formation discussed below (Figure I-7). Polarity is initially established through activation of LKB1, a serine/threonine kinase that is the mammalian PAR-4 ortholog; this activation is sufficient to polarize isolated intestinal epithelial cells (Baas et al., 2004). LKB1 activates PAR-1, another serine/threonine kinase, which causes it to move to the basolateral domain (Karner et al., 2006). In this region, PAR-1 phosphorylates apical components, such as PAR-3, to inactivate them and prevent recruitment of other apical proteins (Benton and Johnston, 2003).

In the apical domain, non-phosphorylated PAR-3 localizes to the TJ, where it forms a complex with both PAR-6 and PRKCZ (Karner et al., 2006). However, this complex is inactive until recruitment of both PTEN (involved in $PIP_2$ synthesis (Martín-Belmonte et al., 2007)) and CDC42. This relieves the baseline inhibition of PRKCZ by PAR-6 (Chen et al., 2013). When active, PRKCZ acts similarly to PAR-1 in the basolateral region, as it phosphorylates basolateral components, such as PAR-1, to exclude them from the apical region (Chen and Zhang, 2013; Karner et al., 2006). Mutations that prevent this complex from forming disrupt polarity (Horikoshi et al., 2009), and mutations in PRKCZ result in mislocalization of junctional and

basolateral components, including ZO1, E-cadherin (CDH1), and spindle orientation proteins (Nelson, 2003; Rodriguez-Boulan and Macara, 2014). Correct orientation of the spindle is important for maintenance of epithelial polarity; for example, in a pseudostratified epithelium, spindle angle control ensures that each daughter cell maintains an apical and basal contact (Meyer et al., 2011).

**Lumen Formation**

A key component to the function of many organs such as the small intestine, lung, kidney, and pancreas is the presence of a patent lumen surrounded by a properly polarized and tightly sealed epithelial layer. This allows for fluids such as air, food, or digestive juices to move within the body while also preventing molecules from entering incorrect body compartments. In the intestinal lumen, ingested food is digested and molecular building blocks are absorbed, while large molecules and pathogens are excluded (Datta et al., 2011).

Lumens may arise from a wide variety of mechanisms. Here we will introduce secondary or *de novo* lumen formation, classically associated with intestinal development (Mathan et al., 1976), lumen formation concurrent with cytokinesis, best described in the zebrafish neural keel (Buckley et al., 2013; Tawk et al., 2007) and *in vitro* cyst formation (Datta et al., 2011; Jaffe et al., 2008), and tissue invagination, focusing on recent developments in the *Drosophila* leg disc (Monier et al., 2015) and tracheal placode (Kondo and Hayashi, 2013) (Figure I-8).

De novo *lumen formation in morphogenesis*

Lumens may form *de novo* within a stratified epithelium. This process occurs in the zebrafish intestine (Andrew and Ewald, 2010; Datta et al., 2011) and the mammalian thyroid

follicle (Hick et al., 2013) and pancreatic acini (Villasenor et al., 2010). In all of these systems, apical components are specifically targeted to sites within the epithelium, appearing initially as polarized spots. Over time, these spots fuse together into a continuous, expansive structure (Figure I-8A.i).

Classically, it was thought that the small intestine developed via a similar process. These *de novo* lumens, called secondary lumens, were believed to form within the stratified epithelium and fuse together to carve out villi (Mathan et al., 1976). However, we now know that isolated lumens do not form in the small intestine during the formation of villi; careful analysis of 3D reconstructions of the developing intestine show a continuous lumen before, during, and after villus morphogenesis (Grosse et al., 2011). Therefore, other mechanisms by which lumens can extend need to be evaluated in this context.

*Lumen formation concurrent with cytokinesis*

Lumens may also be generated by co-opting the process of cell division. *In vivo*, this occurs during formation of the zebrafish neural tube (which contains a central lumen) from the neural keel (a solid rod of cells with no lumen). This lumen forms due to a specialized "crossing" or (c-) division (Tawk et al., 2007). As cells undergo this type of division at the tissue midline, apical components, such as Pard3, and centrosomes are localized to the cytokinetic plane (Figure I-8A.ii). Blocking mitosis dramatically lowers lumen formation efficiency and results in a discontinuous structure (Buckley et al., 2013).

A better understanding of the connection between cytokinesis and lumen formation has come from analysis of multiple *in vitro* systems. Both MDCK.2 and Caco2 cell lines, derived from canine kidney and human intestinal adenoma, respectively, are extensively used to study

three-dimensional cyst formation (Datta et al., 2011; Jaffe et al., 2008). When these cell lines are plated as single cells within a three-dimensional matrix, they form a fully delineated TJ-lined lumen upon the first cell division; subsequent cell divisions increase the size of these cysts (Bryant et al., 2010).

Initially, the cytokinetic plane in these dividing cells is marked by an apical membrane initiation site (AMIS). This forms through trafficking of apical proteins, such as podocalyxin and CRB3, in RAB11A endosomes from the outer edge of the cell (facing the extracellular matrix) along the mitotic spindle to the cytokinetic plane (Schlüter et al., 2009). These endosomes are targeted by the Rho family of GTPases, which interact with apical polarity markers CDC42, PAR-3, and PRKCZ (Apodaca, 2010; Bryant et al., 2010; Rodríguez-Fraticelli et al., 2011). RAB11A appears indispensible for proper lumen formation both *in vitro* and *in vivo*, as its loss results in improper lumen formation (Desclozeaux et al., 2008) and perturbed villus morphogenesis (Yu et al., 2014).

In addition to the importance of endocytic tracking in initiating properly polarized lumens, mitotic spindle orientation is critical for *in vitro* cyst growth. This is controlled by CDC42 and PRKCZ, proteins that are also important for defining apical polarity as described above. CDC42 orients the mitotic spindle, allowing for maintenance of a single, central lumen in Caco2 cysts beyond the two-cell stage (Jaffe et al., 2008). PRKCZ phosphorylates the LGN-NUMA1 spindle orientation complex. This excludes the LGN-NUMA1 complex from the apical surface, preventing cell division from being oriented in the apical-basal direction, and ensures that each daughter cell maintains both an apical and basal surface (Zheng et al., 2010).

Recently, Caco2 cyst formation has been utilized to explore determine the importance of Ezrin and NF2 (Merlin), an Ezrin-associated protein, in spindle angle control (Hebert et al.,

2012). When either of these proteins is improperly localized, spindle orientation is randomized and cysts with multiple lumens form (Hebert et al., 2012). Interestingly, in the adult intestine, loss of Ezrin also results in incorrectly oriented spindles (Casaletto et al., 2011).

While transformed cell lines, such as MDCK and Caco2, are commonly utilized for the study of lumen formation, recent work has shown that single human embryonic stem cells (hESC) also form an AMIS and a lumen during the initial cell division. Interestingly, these cells do not require 3D culture conditions for lumen formation and can also form lumens when grown on a stiff 2D matrix (Taniguchi et al., 2015). Further study of the factors important for proper formation of lumens in this system may yield insight as to how to utilize hESC or induced pluripotent stem cells (iPSC) for the generation of hollow organs, such as the intestine.

*Lumen extension via tissue invagination*

Invagination of an already polarized epithelial sheet is another mechanism to increase lumenal surface area. This process often involves active or passive shape changes within the invaginating epithelial cells. One of the most common mechanisms of translating cellular shape changes into tissue-level morphology changes is through constriction of the apical domain of specific cells in an epithelial sheet. Such mechanisms have been classically studied in many morphogenic processes, ranging from early gastrulation (Odell et al., 1981) to, more recently, the *Drosophila* leg disc (Monier et al., 2015) and tracheal placode (Kondo and Hayashi, 2013). The intracellular forces that accompany these changes will be further discussed in the next section; here, we will focus on the tissue-level changes that occur during lumen extension of *in vivo* systems.

In the *Drosophila* leg disc, apoptotic cells generate an apical to basal intracellular actin-myosin cables, which exert a transient downward pulling force on the junctional complexes, promoting the infolding of neighboring cells (Figure I-8B.ii). Modeling this process *in silico* suggests that both patterned apoptosis throughout the leg disc and propagation of forces generated by this apoptosis are necessary for significant tissue morphology changes; if either of these events do not occur, invagination is inhibited (Monier et al., 2015). Apoptosis is also important for neural tube closure in the early neural ectoderm; inhibiting apoptosis results in tube closure, but with impaired efficiency. The mechanism by which apoptosis generates these shape changes has yet to be elucidated, although intraepithelial forces may be at work (Yamaguchi and Miura, 2012; Yamaguchi et al., 2011).

In addition to apoptosis, mitosis can generate tissue-level forces and morphological changes that can result in tissue invagination. In the *Drosophila* trachea, a two-step process increases lumenal surface (Figure I-8B.i). First, EGF signaling causes epithelial cell intercalation in a field of cells that surround the presumptive tracheal placode, circumferentially constricting cells of the placode. In the context of this centripetal force, cell divisions within these constricted regions results in rapid (within minutes) tissue invagination (Nishimura et al., 2007). Additionally, the rounded mitotic cells have a characteristic and unusual feature in that they enter mitosis well inside the epithelium ("internalized cell rounding") and remains connected to the overlying apical surface by a T-shaped apical membrane extension.

Interestingly, such invaginations do not require cell division itself, but cell rounding prior to mitosis is sufficient (Kondo and Hayashi, 2013). This is highlighted by treating the tissue with the small molecule colchicine, which irreversibly arrests cells at the G2/M transition while still allowing mitotic rounding to occur (Zieve et al., 1980). Even with this treatment, invagination

occurs efficiently. As with apoptosis in the leg disc, intraepithelial forces are transmitted via Myosin II (Kondo and Hayashi, 2013). Thus far, the *Drosophila* trachea is the only known system in which shape changes during mitosis promote lumenal expansion.

Invagination in the tracheal placode also requires that the surrounding constriction of the invaginating cells is passive; if, in contrast, mitotic cell rounding occurs in the context of active apical constriction, this will interfere with rather than promote invagination (Kondo and Hayashi, 2013).

**Physical Forces and Morphogenesis**

As is highlighted by the process of *Drosophila* tracheal placode invagination described above, tissue forces, such as the patterned passive constriction of cells in this epithelium, can assist and pattern morphogenic events. Tissue structure characteristics (such as extracellular matrix stiffness) can alter the distribution of both signaling molecules and mechanical forces, which can change cell behavior (Nelson and Gleghorn, 2012). Here, we consider the effects of active cell shape changes and volume redistribution on tissue morphogenesis as well as the effects of intraepithelial strain on spindle orientation and tissue growth.

*Factors changing cell shape*

Changes within single cells can be propagated to generate global tissue shape modifications. Myosin II activity as well as cytoplasmic volume distribution can cause such changes (Kondo and Hayashi, 2015). Contraction of Myosin II pulls on actin filaments to apically or basally constrict cells, thereby exerting intraepithelial forces via the junctional connections between cell neighbors (Martin and Goldstein, 2014). The distribution of Myosin II

at the apical, basal, and lateral surfaces of epithelial cells can alter cell shape. For example, apical constriction, often a precursor to tissue invagination, occurs by Myosin II constriction modulated by Rho kinase activity (Kondo and Hayashi, 2015).

Additionally, redistribution of cytoplasm within the cell can exert pressure on the cell membrane and change cell shape (He et al., 2014; Polyakov et al., 2014). Nevertheless, each cell's total volume usually remains constant during morphogenesis (Odell et al., 1981). The only morphogenic change that is well documented to involve a change in cell volume is cell rounding prior to mitosis, which increases cell volume by up to 30%. Even this change is transient; after mitosis, the cells return to their original size (Zlotek-Zlotkiewicz et al., 2015).

These forces are often transmitted through tissues through the action of AJ (Röper, 2015; Takeichi, 2014). One key component of AJ allowing for force transmission is α-catenin, which, when under increased tension, undergoes a conformational change to allow binding of Vinculin; this binding increases contact with the actin cytoskeleton and results in more efficiently transduced forces across the AJ (Nelson and Gleghorn, 2012; Yonemura et al., 2010). If AJs are lost, instead of producing morphological changes, forces within the tissue will result in tearing, further emphasizing the importance of intact junctions in this process (Martin et al., 2010).

*External forces affect cell division and tissue shape*

External forces on cells can affect both their cell biology, such as how they undergo mitosis, and the morphology of developing tissues. For isolated cells, spindle orientation depends on cell geometry as well as external constraints on the dividing cell. Sea urchin zygotes singly plated in differently shaped wells orient their mitotic spindle depending on the shape of the well in which they are plated. In this microtubule-dependent process, these cells first find their center

of mass and then elongate their nuclei along the long axis of the cell (Minc et al., 2011). External forces applied to single human cells can also align the mitotic spindle through changing the sub-cortical actin distribution of these cells (Fink et al., 2011). Cultured cells in a monolayer also are affected by the surrounding forces; cells on the edge (under the most tension) proliferate at a faster rate than the surrounding cells (Nelson et al., 2005).

Further changes in the cell biology of mitosis have been observed in the zebrafish embryo during epiboly, when the enveloping cell layer (EVL, an epithelial sheet) extends over the yolk sac. Proper expansion of the epithelium depends on the correct orientation of cell division (Campinho et al., 2013). Similarly to results described in single cells, the shape of the dividing cell affects spindle angle. In addition to this microtubule-mediated mechanism, a separate, Myosin II-dependent mechanism affects how cells divide. Myosin II, as described above, is important for transducing forces throughout epithelia. Blocking the activity of this motor protein with blebbistatin, a Myosin II inhibitor, changes spindle angle and prevents proper EVL expansion (Campinho et al., 2013). This highlights the importance of intraepithelial forces in affecting the behavior of individual cells.

Proper growth of the *Drosophila* wing disc also depends on epithelial forces. In this system, internal cells of the wing disc proliferate faster than the external cells, causing an increased force along this boundary. The amount and orientation of cell division in the outer region of the wing disc depends on the non-cell autonomous compression forces originating from expansion of the inner cells (Li et al., 2012). Ectopically increasing proliferation in this internal region increases the force on the external cells, altering their cell division orientation and growth pattern of cell clones. In turn, changes in tissue shape are observed (Mao et al., 2013). Proliferation rate can also be affected by these tissue-wide forces (Rauskolb et al., 2014).

Therefore, in this system, similarly to the zebrafish EVL, intraepithelial forces affect tissue morphogenesis.

*Tissue forces as developmental mechanisms*

The role that intraepithelial forces play in causing tissue-level morphological changes is relatively unexplored within developmental biology, especially in higher model organisms such as mice. Gene expression, chemical signaling, and morphogen gradients are often considered to be the main factors affecting tissue morphogenesis. The studies that translate forces exerted on cells within an epithelium into biological changes that affect tissue structure provide a new lens with which to view the complicated process of development.

Understanding these more complicated processes is often facilitated by *in silico* modeling of intraepithelial forces. One of the first cases in which modeling was used to understand morphogenesis was early gastrulation and ventral furrow formation in *Drosophila* (Odell et al., 1981). Many of these models place a strong emphasis on the role that cell shape changes play in force transmission to neighboring cells; using these systems, it is possible to see how such changes are sufficient for tissue-wide morphological changes like invagination (Figure I-9A) (Gelbart et al., 2012; He et al., 2014; Odell et al., 1981). Even though cell shape may dramatically change during development, many of these models are based on the assumption that the overall cell volume remains constant (Gelbart et al., 2012; He et al., 2014; Odell et al., 1981; Polyakov et al., 2014). Recently, this assumption that cells tightly control their volume during morphogenesis has been further confirmed using live imaging (Khan et al., 2014).

In addition to cell shape changes, another parameter commonly shown to affect morphogenesis *in silico* is apical and basal tension. For example, increasing apical tension, as

occurs during apical constriction, while maintaining a constant basal tension causes the epithelium to bend upward (Figure I-9B) (Krajnc et al., 2013). Decreasing basal rigidity can also cause tissue invagination in an apically constricted tissue (Polyakov et al., 2014). *In silico*, invagination has been shown to result from patterned intraepithelial forces (Hannezo et al., 2014). As described in the *Drosophila* wing disc, these forces may arise from cell shape changes or increased cell divisions (Mao et al., 2013); these are sufficient to buckle the tissue into folds (Hannezo et al., 2014).

*In vivo* analyses of biological changes during morphogenesis have resolved many questions about morphogenic events that accompany development. However, such analyses taken alone often ignore the mechanical effects that are mediated by changes in cell shape, differential regions of proliferation, or alterations in orientation of cell division. As a result of the work in this thesis, we have seen how *in silico* modeling of villus morphogenesis can provide a useful strategy to explore how tissue forces can dynamically affect the developing intestine. Integration of our biological studies with *in silico* modeling has provided a deeper understanding of how signaling and tissue forces work together to effect a morphological change.

**Goals of this Thesis Work**

The overarching goal of these investigations has been to understand how intestinal villi are generated and expand apical surface area. Chapter II integrates biological studies with *in silico* modeling to explore how the pattern of mesenchymal clusters can be transferred, via tissue forces, to the epithelium to generate a series of apical invaginations that define the first villi. In Chapter III, we explore the fused villi and ectopic lumens observed in the *Ezrin* null mouse model, revealing several new aspects of this phenotype that shed light onto normal villus

morphogenesis. Together, as described in the concluding chapter, these studies improve our understanding of the interplay between physics and biology in intestinal morphogenesis and generate exciting new questions for future explorations.

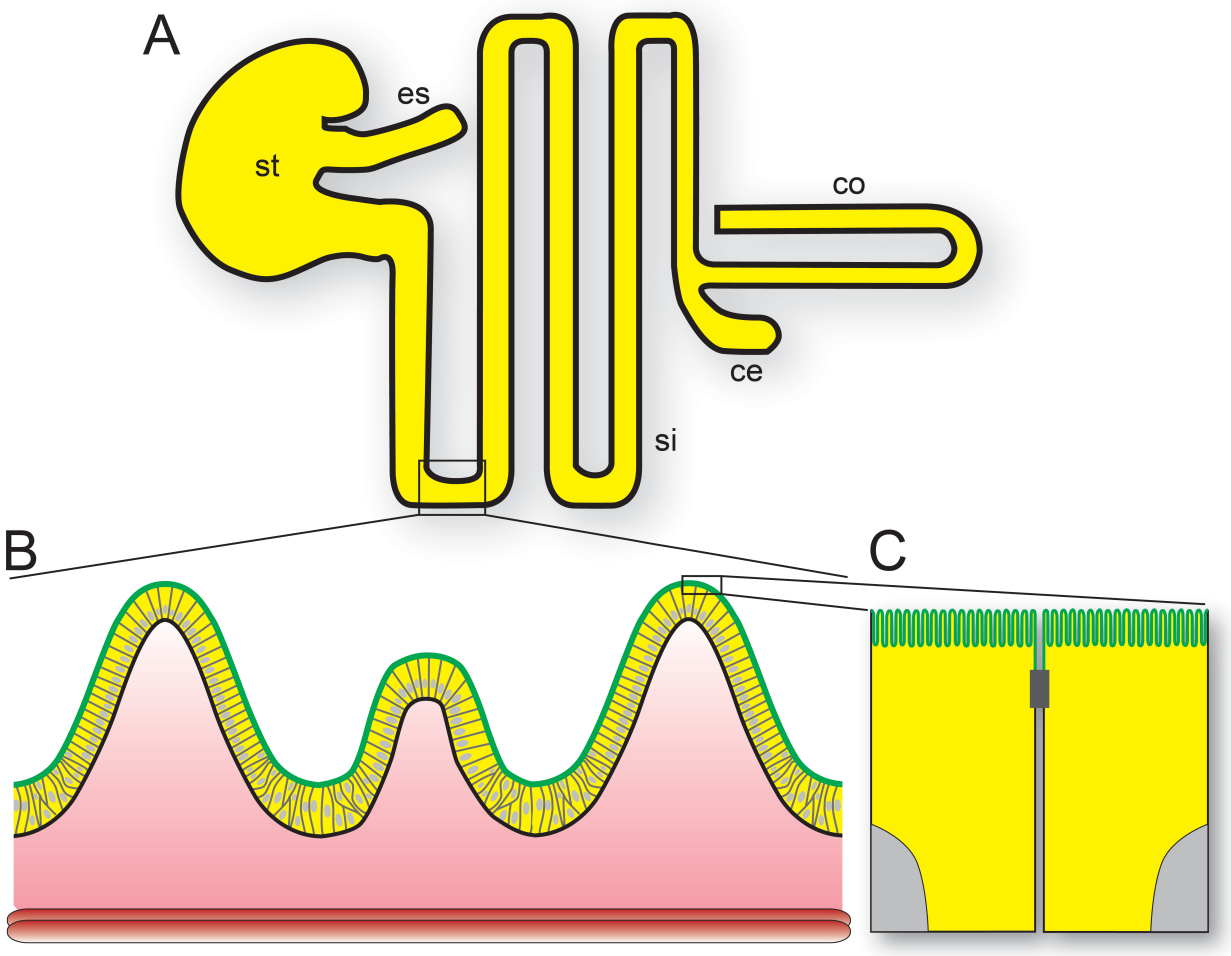


**Figure I-1. The intestine uses multiple mechanisms to increase surface area.** (A) The overall structure of the gastrointestinal tract, including the esophagus (es), stomach (st), small intestine (si), cecum (ce), and colon (co). (B) The intestinal surface is studded with villi, fingerlike projections of epithelium (yellow) lined with an apical surface (green), each containing a mesenchymal core (pink). The whole intestinal tube is surrounded by smooth muscle (red). Villi increase surface area by about 6.5 times compared with a flat surface. (C) The apical surface of each absorptive cell of the intestinal epithelium is further convoluted with microvilli, further increasing the absorptive surface area by about 13 times. Proper development of all three of components is required for proper growth, development, and homeostasis. (Adapted from Walton et al., 2016, Submitted)

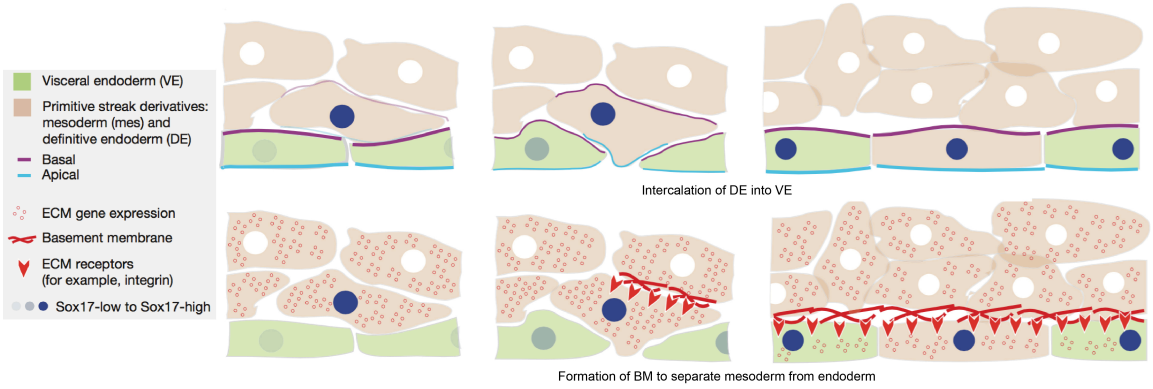


**Figure I-2. Endoderm has a dual embryonic origin.** The endoderm is derived from both the visceral endoderm (VE), classically considered an extra-embryonic tissue, and the definitive endoderm (DE). During gastrulation, the DE intercalates between cells of the VE, after which polarity of the endoderm is established, junctional complexes form between epithelial cells, and the basement membrane forms along the basal surface of this cell layer, which now expresses the endoderm marker SOX17. (Adapted with permission from Viotti et al., 2014)

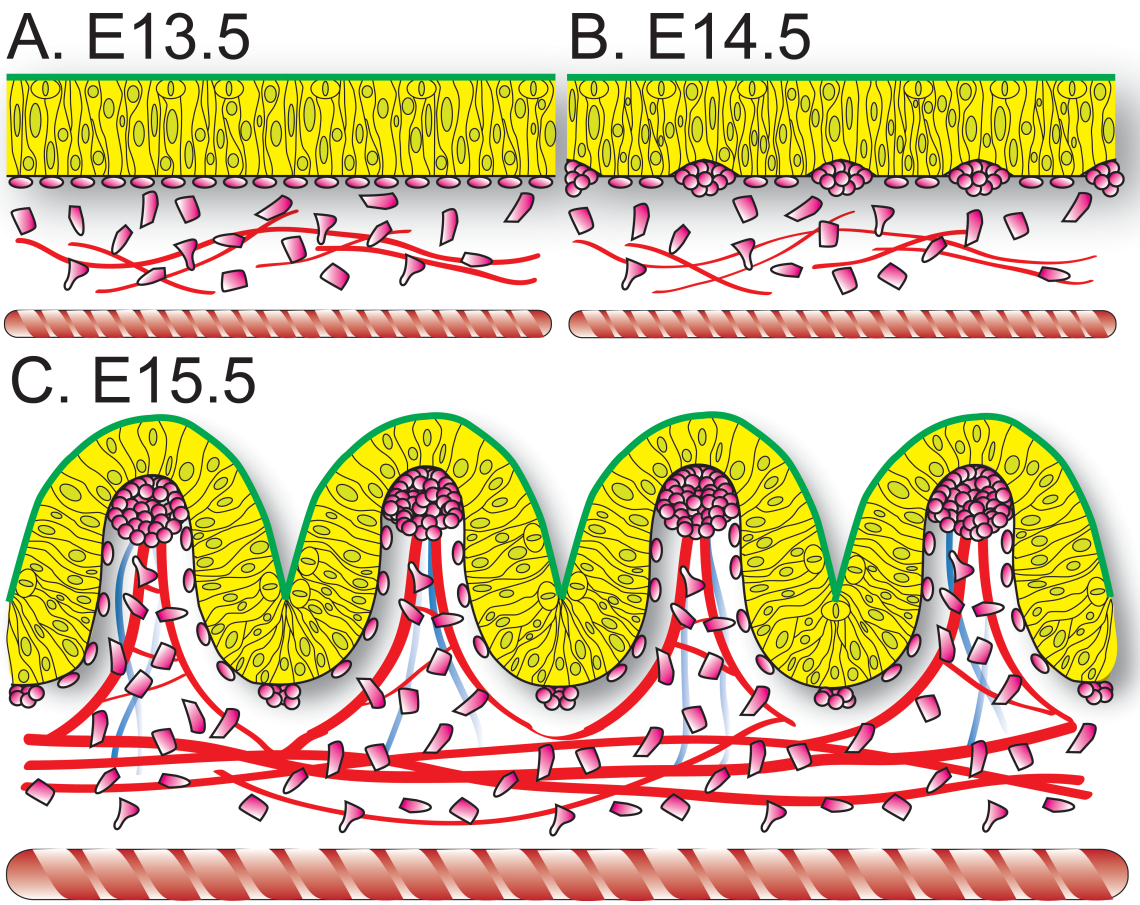


**Figure I-3. Epithelial structure dramatically changes during villus morphogenesis.** The intestinal epithelium changes dramatically from embryonic day (E)13.5 to E15.5. (A) At E13.5, the epithelium is pseudostratified and has a flat apical surface (green). (B) At E14.5, mesenchymal clusters (pink) coalesce adjacent to the basement membrane of the epithelium and deform the overlying cells, while the apical surface remains flat. (C) At E15.5, villi are demarcated and beginning to extend into the lumen. New mesenchymal clusters form at the base of the villi to initiate the later rounds of villus formation. Note the presence of the muscle (red) throughout, along with the close association of blood vessels (bright red) and the developing villi. (Adapted from Walton et al., 2016, Submitted)

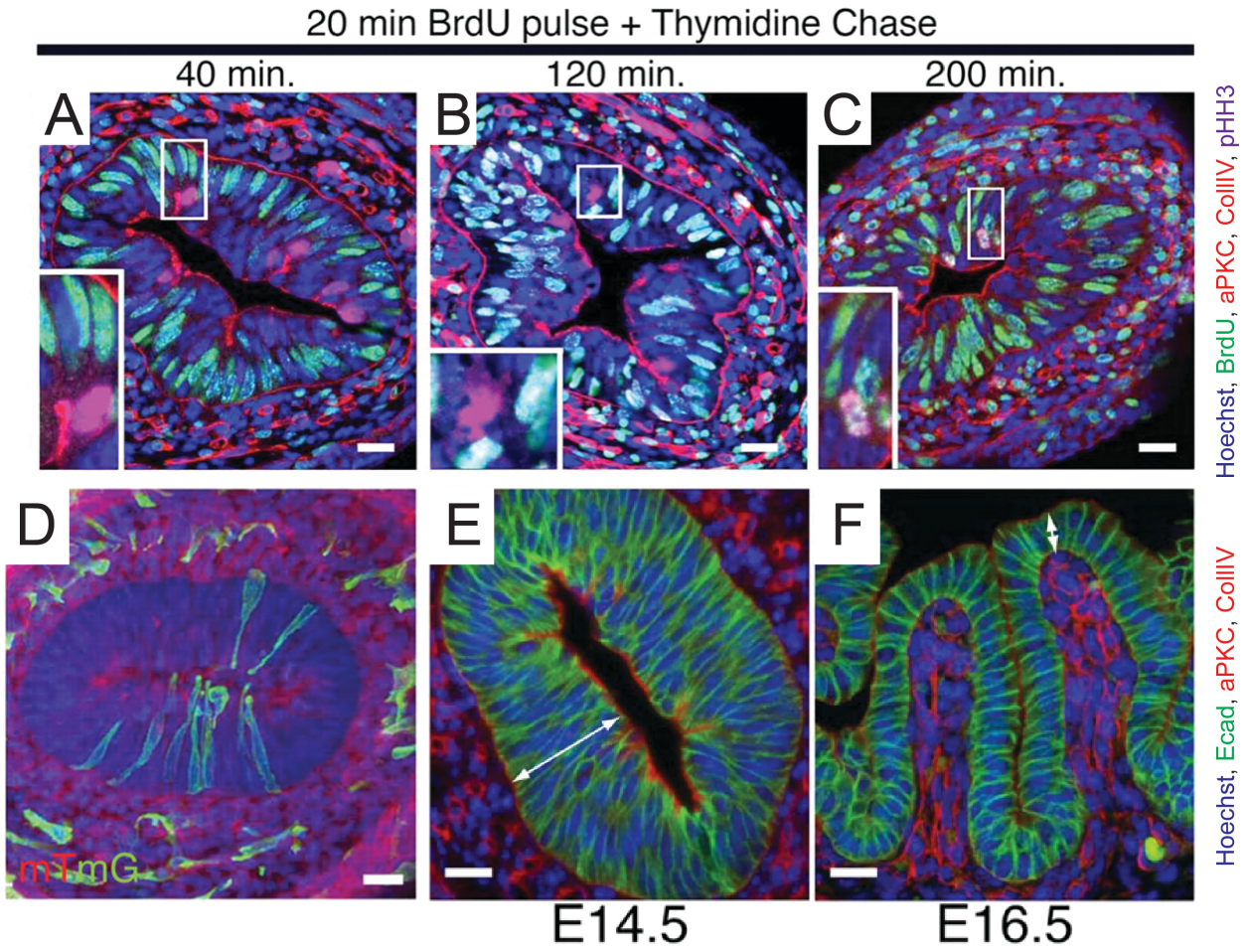


**Figure I-4. The early intestinal epithelium is pseudostratified and undergoes interkinetic nuclear migration.** (A-C) At E14.5, mice were injected with a 20 minute pulse of bromodeoxyuridine (BrdU) to label cells synthesizing DNA. Intestines were harvested after (A) 40 minutes, (B) 120 minutes, or (C) 200 minutes to observe the movement of the labeled cells. This analysis shows that cells synthesize DNA at the basement membrane (Collagen IV, red) and move up towards the apical surface (aPKC, red), where they undergo mitosis (pHH3, purple). This is characteristic of cells undergoing interkinetic nuclear migration (IKNM). (D) 100 μm thick cross-section of an intestine at E14.5, labeling individual cells using the *Cagg-CreER*$^{TM}$*;mTmG* system. Note how almost all cells touch both the apical and basal surfaces. (E-F) Changes in epithelial structure before (E) and after (F) villus formation. Note the cell borders (E-cadherin, green): the pre-villus epithelium contains very tall and narrow cells, while after villi form the cells become columnar. Apical surface (aPKC, red) also greatly expands during this time. (Adapted with permission from Grosse et al, 2011)

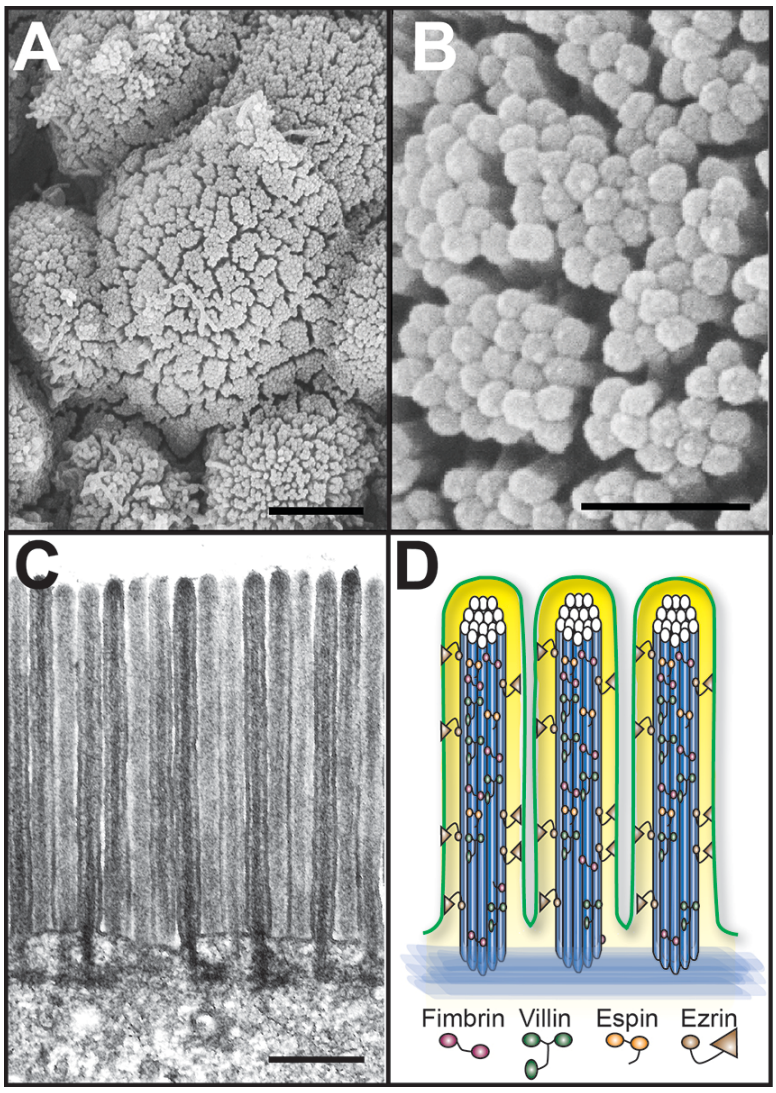


**Figure I-5. Microvilli further convolute the absorptive surface of the intestine.** (A-B) Scanning electron micrographs (SEM) of the apical surface at E15.5 shows a field of microvilli at low (A, scale bar 2 μm) and high (B, scale bar 500 nm) magnification. (C) Transmission electron micrograph (TEM) of microvilli at E15.5. Note the apical terminal web at the base of the microvilli and the actin core seen within each microvillus (scale bar 500 nm). (D) Schematic of microvillus structure, highlighting the actin core (blue rods), along with major structural proteins that bundle these fibers together (fimbrin, villin, espin), and Ezrin, which connects to the apical surface (green). (Adapted from Walton et al., 2016, Submitted)

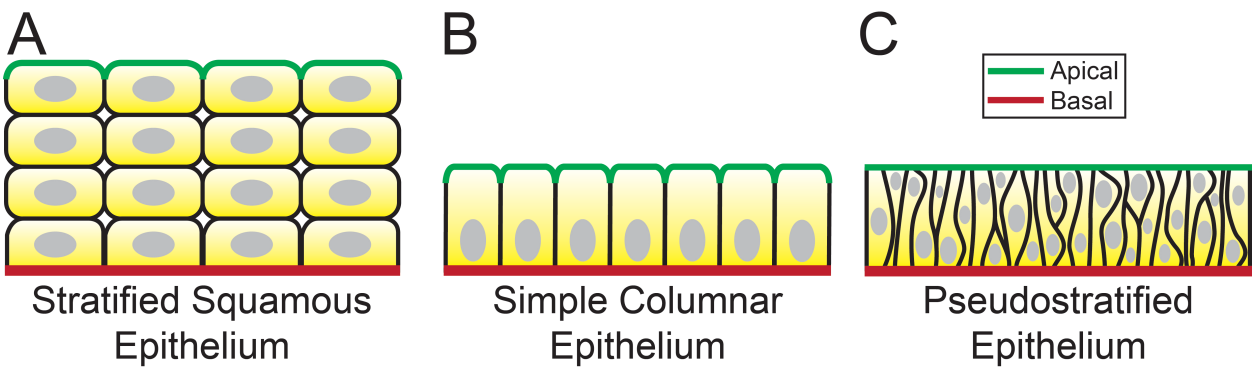


**Figure I-6. Epithelia have a wide variety of structures.** Epithelia are characterized as having an apical (green) and basal (red) surface. They can be categorized based on cell shape and layer arrangement. Some examples include a (A) stratified squamous epithelium, with multiple layers of flattened cells, (B) simple columnar epithelium, with a single layer of tall, thin cells), and (C) pseudostratified epithelium, with a single layer of tightly packed cells with varying shapes and staggered nuclei.

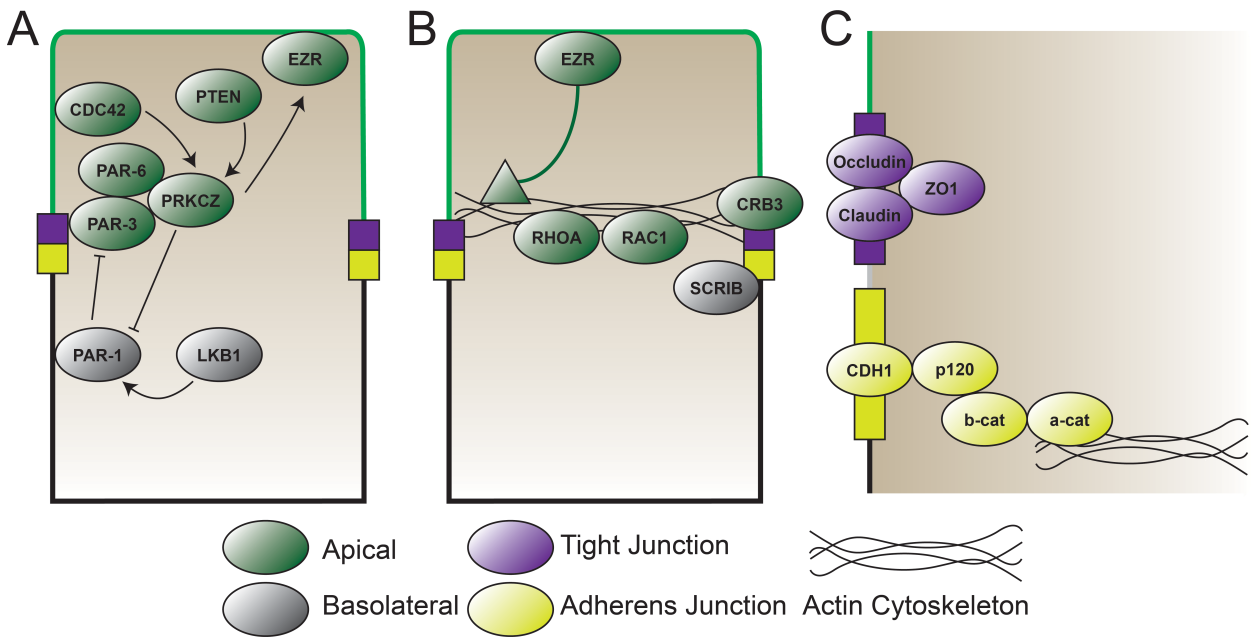


**Figure I-7. Essential components of the cell polarity machinery.** The apical (green) and basolateral (black) surfaces are separated by junctional complexes. This summarizes the main proteins involved in establishing and maintaining polarity, along with their interactions (summarized further in the text). (A) LKB1 activates PAR-1, which excludes PAR-3 and other apical components from the basolateral region. PAR-3 forms a complex with PAR-6 and PRKCZ, which is activated by PTEN and CDC42 to exclude basolateral components from the apical region. PRKCZ (aPKC) also activates EZR. (B) EZR attaches to the actin cytoskeleton, which also recruits RHOA and RAC1. CRB3 is a transmembrane protein localized to the apical domain and SCRIB localizes on the basolateral side of the junction. (C) Cell-cell junctional complexes, defined by the tight (purple) and adherens (yellow) junctions. These consist of transmembrane components (Occludins, Claudins, and CDH1) and proteins that attach to these components (ZO1, p120, β-catenin, α-catenin). Note that α-catenin also attaches to the actin cytoskeleton.

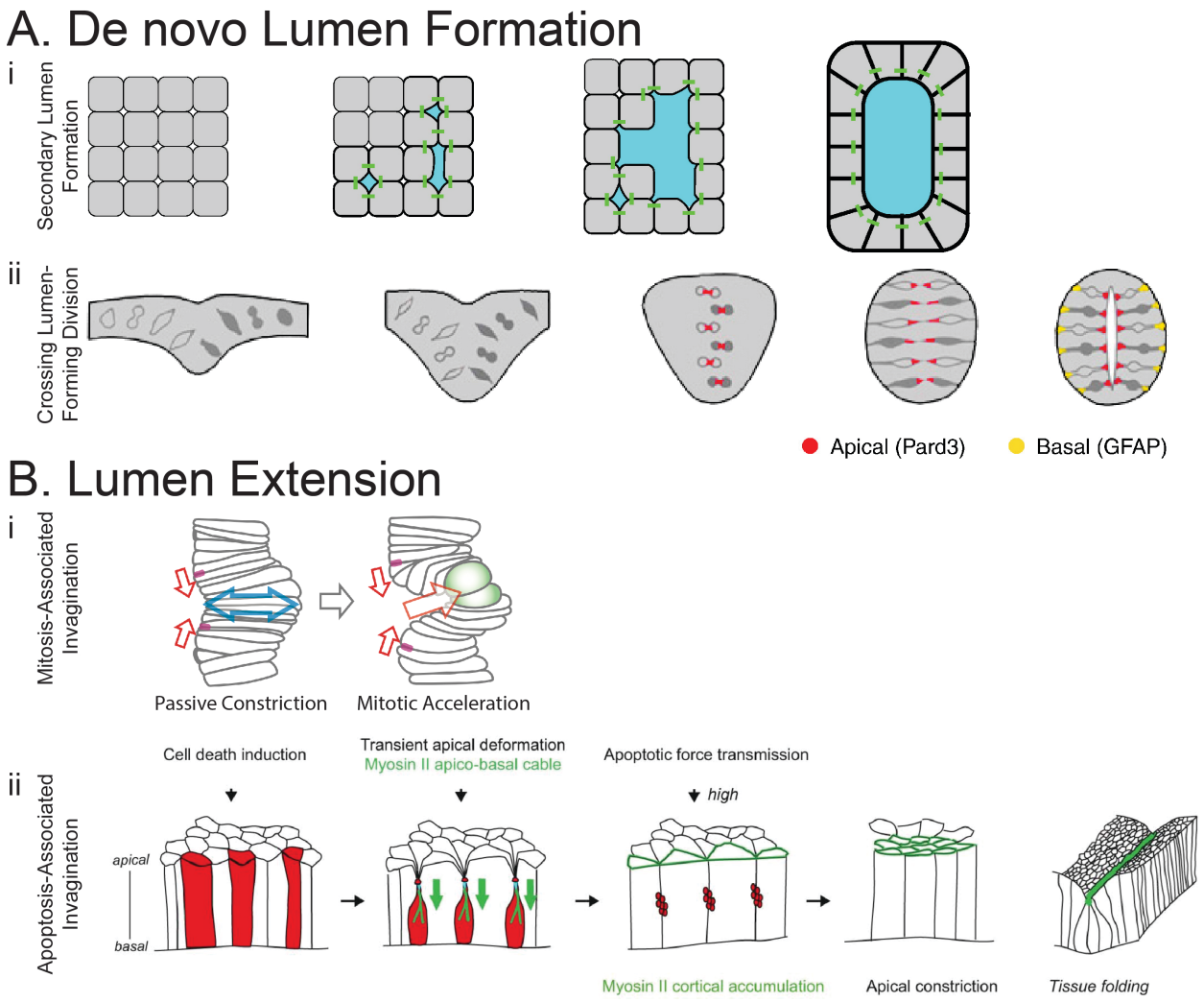


**Figure I-8. Lumens form and extend by a variety of mechanisms.** (A) Lumens may form *de novo* by secondary lumen formation (i), in which the lumen (blue) is defined within a stratified epithelium and surrounded by junctions (green), or a cell division (ii), as occurs in the zebrafish neural keel to deposit apical components (red) at the midline of the keel to form the neural tube. (B) Lumens may also extend from an existing structure. (i) In the *Drosophila* tracheal placode, passive constriction of specific regions by patterned cell intercalation first occurs. Then, mitotic cell rounding accelerates the deepening of the invagination and apical surface extension. (ii) In the *Drosophila* leg disc, patterned apoptosis exerts a transient force on the surrounding cells, allowing them to undergo apical constriction, which increases the efficiency of tissue folding. (Adapted with permission from Andrew and Ewald, 2010; Kondo and Hayashi, 2013; Monier et al, 2015)

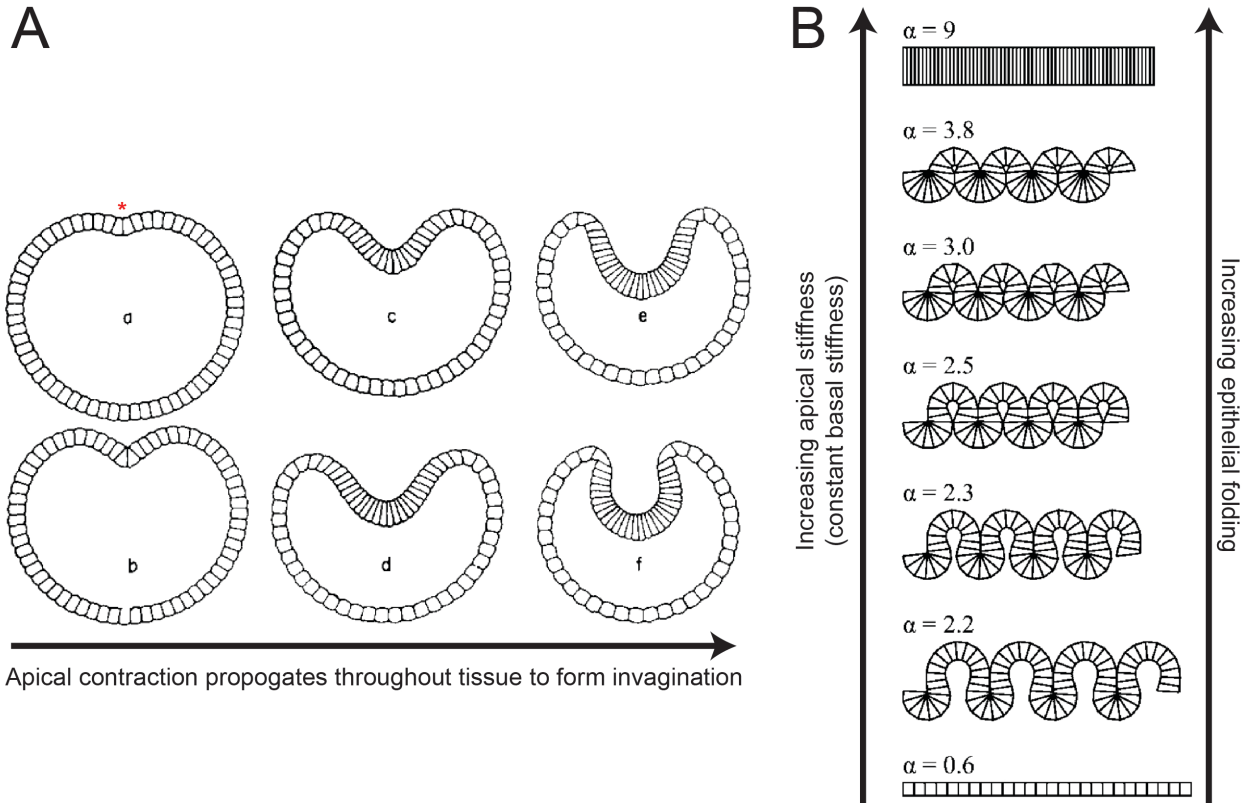


**Figure I-9. *In silico* modeling greatly aids the understanding of the role of physical forces in tissue shape changes during morphogenesis.** (A) Model of early gastrulation, in which an initial apical constriction is found to spread in a "wave-like" pattern around the spherical embryo. This causes efficient invagination of a patch of the embryo. (B) Effect of changing physical properties of the epithelium. Increasing apical stiffness ($\alpha$) while maintaining a constant basal stiffness ($\beta$) allows for changing shape of the cells within the epithelium from cuboidal to columnar. In addition to individual cell shape changes, the overall shape of the epithelium changes; increasing $\alpha$ tightens these convolutions. (Adapted with permission from Odell et al., 1981; Krajnc, et al., 2013)

**Literature Cited**


**Andrew, D. J. and Ewald, A. J.** (2010). Morphogenesis of epithelial tubes: Insights into tube formation, elongation, and elaboration. *Developmental Biology* **341**, 34–55.

**Apodaca, G.** (2010). Opening ahead: early steps in lumen formation revealed. *Nature Cell Biology* **12**, 1026.

**Baas, A. F., Kuipers, J., van der Wel, N. N., Batlle, E., Koerten, H. K., Peters, P. J. and Clevers, H. C.** (2004). Complete polarization of single intestinal epithelial cells upon activation of LKB1 by STRAD. *Cell* **116**, 457–466.

**Bartles, J. R., Zheng, L., Li, A., Wierda, A. and Chen, B.** (1998). Small Espin: A Third Actin-bundling Protein and Potential Forked Protein Ortholog in Brush Border Microvilli. *The Journal of Cell Biology* **143**, 107–119.

**Benton, R. and Johnston, D. S.** (2003). Drosophila PAR-1 and 14-3-3 Inhibit Bazooka/PAR-3 to Establish Complementary Cortical Domains in Polarized Cells. *Cell* **115**, 691–704.

**Berryman, M., Franck, Z. and Bretscher, A.** (1993). Ezrin is concentrated in the apical microvilli of a wide variety of epithelial cells whereas moesin is found primarily in endothelial cells. *J. Cell. Sci.* **105 ( Pt 4)**, 1025–1043.

**Braunger, J. A., Brueckner, B. R., Nehls, S., Pietuch, A., Gerke, V., Mey, I., Janshoff, A. and Steinem, C.** (2014). Phosphatidylinositol 4,5-bisphosphate alters the number of attachment sites between ezrin and actin filaments: a colloidal probe study. *Journal of Biological Chemistry*.

**Bretscher, A., Edwards, K. and Fehon, R. G.** (2002). ERM proteins and merlin: integrators at the cell cortex. *Nat Rev Mol Cell Biol* **3**, 586–599.

**Brückner, B. R., Pietuch, A., Nehls, S., Rother, J. and Janshoff, A.** (2015). Ezrin is a Major Regulator of Membrane Tension in Epithelial Cells. *Scientific Reports* **5**, 14700.

**Bryant, D. M., Datta, A., Rodríguez-Fraticelli, A. E., Peränen, J., Martín-Belmonte, F. and Mostov, K. E.** (2010). A molecular network for de novo generation of the apical surface and lumen. *Nature Cell Biology* **12**, 1035–1045.

**Buckley, C. E., Ren, X., Ward, L. C., Girdler, G. C., Araya, C., Green, M. J., Clark, B. S., Link, B. A. and Clarke, J. D. W.** (2013). Mirror-symmetric microtubule assembly and cell interactions drive lumen formation in the zebrafish neural rod. *The EMBO Journal* **32**, 30–44.

**Burgess, D. R.** (1975). Morphogenesis of intestinal villi II. Mechanism of formation of previllous ridges. *Development* **34**, 723–740.

**Burtscher, I. and Lickert, H.** (2009). Foxa2 regulates polarity and epithelialization in the endoderm germ layer of the mouse embryo. *Development* **136**, 1029–1038.

**Campinho, P., Behrndt, M., Ranft, J., Risler, T., Minc, N. and Heisenberg, C.-P.** (2013). Tension-oriented cell divisions limit anisotropic tissue tension in epithelial spreading during zebrafish epiboly. *Nature Cell Biology* **15**, 1405–1414.

**Casaletto, J. B., Saotome, I., Curto, M. and McClatchey, A. I.** (2011). Ezrin-mediated apical integrity is required for intestinal homeostasis. *Proc. Natl. Acad. Sci. U.S.A.* **108**, 11924–11929.

**Chen, C.-T., Ettinger, A. W., Huttner, W. B. and Doxsey, S. J.** (2013). Resurrecting remnants: the lives of post-mitotic midbodies. *Trends in Cell Biology* **23**, 118–128.

**Chen, J. and Zhang, M.** (2013). The Par3/Par6/aPKC complex and epithelial cell polarity. *Experimental Cell Research* **319**, 1357–1364.

**Clarke, R.** (1967). On the constancy of the number of villi in the duodenum of the post-embryonic domestic fowl.

**Datta, A., Bryant, D. M. and Mostov, K. E.** (2011). Molecular Regulation of Lumen Morphogenesis. *Current Biology* **21**, R126–R136.

**Desclozeaux, M., Venturato, J., Wylie, F. G., Kay, J. G., Joseph, S. R., Le, H. T. and Stow, J. L.** (2008). Active Rab11 and functional recycling endosome are required for E-cadherin trafficking and lumen formation during epithelial morphogenesis. *AJP: Cell Physiology* **295**, C545–C556.

**Ezzell, R. M., Chafel, M. M. and Matsudaira, P. T.** (1989). Differential localization of villin and fimbrin during development of the mouse visceral endoderm and intestinal epithelium. *Development* **106**, 407–419.

**Fath, K. R. and Burgess, D. R.** (1995). Microvillus assembly. Not actin alone. *Curr. Biol.* **5**, 591–593.

**Fehon, R. G., McClatchey, A. I. and Bretscher, A.** (2010). Organizing the cell cortex: the role of ERM proteins. 1–12.

**Ferrary, E.** (1999). In Vivo, Villin Is Required for Ca2+-dependent F-actin Disruption in Intestinal Brush Borders. *The Journal of Cell Biology* **146**, 819–830.

**Fink, J., Carpi, N., Betz, T., Bétard, A., Chebah, M., Azioune, A., Bornens, M., Sykes, C., Fetler, L., Cuvelier, D., et al.** (2011). External forces control mitotic spindle positioning. *Nature Cell Biology* **13**, 771–778.

**Fleming, T. P., Papenbrock, T., Fesenko, I., Hausen, P. and Sheth, B.** (2000). Assembly of tight junctions during early vertebrate development. *Semin. Cell Dev. Biol.* **11**, 291–299.

**Forrester, J. M.** (1972). The number of villi in rat's jejunum and ileum: effect of normal growth, partial enterectomy, and tube feeding. *J. Anat.* **111**, 283–291.

**Franklin, V., Khoo, P. L., Bildsoe, H., Wong, N., Lewis, S. and Tam, P. P. L.** (2008). Regionalisation of the endoderm progenitors and morphogenesis of the gut portals of the mouse embryo. *Mechanisms of Development* **125**, 587–600.

**Gelbart, M. A., He, B., Martin, A. C., Thiberge, S. Y., Wieschaus, E. F. and Kaschube, M.** (2012). Volume conservation principle involved in cell lengthening and nucleus movement during tissue morphogenesis. *Proc. Natl. Acad. Sci. U.S.A.* **109**, 19298–19303.

**Goulet, O. and Ruemmele, F.** (2006). Causes and management of intestinal failure in children. *YGAST* **130**, S16–28.

**Goulet, O., Ruemmele, F., Lacaille, F. and Colomb, V.** (2004). Irreversible intestinal failure. *J. Pediatr. Gastroenterol. Nutr.* **38**, 250–269.

**Grimm-Gunter, E. M. S., Revenu, C., Ramos, S., Hurbain, I., Smyth, N., Ferrary, E., Louvard, D., Robine, S. and Rivero, F.** (2009). Plastin 1 Binds to Keratin and Is Required for Terminal Web Assembly in the Intestinal Epithelium. *Molecular Biology of the Cell* **20**, 2549–2562.

**Grosse, A. S., Pressprich, M. F., Curley, L. B., Hamilton, K. L., Margolis, B., Hildebrand, J. D. and Gumucio, D. L.** (2011). Cell dynamics in fetal intestinal epithelium: implications for intestinal growth and morphogenesis. *Development* **138**, 4423–4432.

**Hampton, C. M., Liu, J., Taylor, D. W., DeRosier, D. J. and Taylor, K. A.** (2008). The 3D structure of villin as an unusual F-actin crosslinker. *Structure*.

**Hannezo, E., Prost, J. and Joanny, J.-F.** (2014). Theory of epithelial sheet morphology in three dimensions. *Proc. Natl. Acad. Sci. U.S.A.* **111**, 27–32.

**He, B., Doubrovinski, K., Polyakov, O. and Wieschaus, E.** (2014). Apical constriction drives

tissue-scale hydrodynamic flow to mediate cell elongation. *Nature* **508**, 392–396.
**Hebert, A. M., DuBoff, B., Casaletto, J. B., Gladden, A. B. and McClatchey, A. I.** (2012). Merlin/ERM proteins establish cortical asymmetry and centrosome position. *Genes & Development* **26**, 2709–2723.
**Helander, H. F. and Fändriks, L.** (2014). Surface area of the digestive tract – revisited. *Scandinavian Journal of Gastroenterology* **49**, 681–689.
**Helmrath, M. A., VanderKolk, W. E., Can, G., Erwin, C. R. and Warner, B. W.** (1996). Intestinal adaptation following massive small bowel resection in the mouse. *J. Am. Coll. Surg.* **183**, 441–449.
**Hick, A.-C., Delmarcelle, A.-S., Bouquet, M., Klotz, S., Copetti, T., Forez, C., Van Der Smissen, P., Sonveaux, P., Collet, J.-F., Feron, O., et al.** (2013). Reciprocal epithelial:endothelial paracrine interactions during thyroid development govern follicular organization and C-cells differentiation. *Developmental Biology* **381**, 227–240.
**Horikoshi, Y., Suzuki, A., Yamanaka, T., Sasaki, K., Mizuno, K., Sawada, H., Yonemura, S. and Ohno, S.** (2009). Interaction between PAR-3 and the aPKC-PAR-6 complex is indispensable for apical domain development of epithelial cells. *J. Cell. Sci.* **122**, 1595–1606.
**Jaffe, A. B., Kaji, N., Durgan, J. and Hall, A.** (2008). Cdc42 controls spindle orientation to position the apical surface during epithelial morphogenesis. *The Journal of Cell Biology* **183**, 625–633.
**Jayasundar, J. J., Ju, J. H., He, L., Liu, D., Meilleur, F., Zhao, J., Callaway, D. J. E. and Bu, Z.** (2012). Open Conformation of Ezrin Bound to Phosphatidylinositol 4,5-Bisphosphate and to F-actin Revealed by Neutron Scattering. *Journal of Biological Chemistry* **287**, 37119–37133.
**Karlsson, L., Lindahl, P., Heath, J. K. and Betsholtz, C.** (2000). Abnormal gastrointestinal development in PDGF-A and PDGFR-(alpha) deficient mice implicates a novel mesenchymal structure with putative instructive properties in villus morphogenesis. *Development* **127**, 3457–3466.
**Karner, C., Wharton, K. A. and Carroll, T. J.** (2006). Apical-basal polarity, Wnt signaling and vertebrate organogenesis. *Semin. Cell Dev. Biol.* **17**, 214–222.
**Kemphues, K. J., Priess, J. R., Morton, D. G. and Cheng, N.** (1988). Identification of genes required for cytoplasmic localization in early C. elegans embryos. *Cell* **52**, 311–320.
**Khan, Z., Wang, Y.-C., Wieschaus, E. F. and Kaschube, M.** (2014). Quantitative 4D analyses of epithelial folding during Drosophila gastrulation. *Development* **141**, 2895–2900.
**Kolterud, A., Grosse, A. S., Zacharias, W. J., Walton, K. D., Kretovich, K. E., Madison, B. B., Waghray, M., Ferris, J. E., Hu, C., Merchant, J. L., et al.** (2009). Paracrine Hedgehog Signaling in Stomach and Intestine: New Roles for Hedgehog in Gastrointestinal Patterning. *Gastroenterology* **137**, 618–628.
**Kondo, T. and Hayashi, S.** (2013). Mitotic cell rounding accelerates epithelial invagination. *Nature* **494**, 125–129.
**Kondo, T. and Hayashi, S.** (2015). Mechanisms of cell height changes that mediate epithelial invagination. *Develop. Growth Differ.* **57**, 313–323.
**Krajnc, M., Štorgel, N., Brezavšček, A. H. and Ziherl, P.** (2013). A tension-based model of flat and corrugated simple epithelia. *Soft Matter* **9**, 8368–8377.
**Kwon, G. S., Viotti, M. and Hadjantonakis, A.-K.** (2008). The endoderm of the mouse embryo arises by dynamic widespread intercalation of embryonic and extraembryonic lineages.

*Developmental Cell* **15**, 509–520.
**Lee, H. O. and Norden, C.** (2013). Mechanisms controlling arrangements and movements of nuclei in pseudostratified epithelia. *Trends in Cell Biology* **23**, 141–150.
**Lewis, S. L. and Tam, P. P. L.** (2006). Definitive endoderm of the mouse embryo: Formation, cell fates, and morphogenetic function. *Developmental Dynamics* **235**, 2315–2329.
**Li, X., Udager, A. M., Hu, C., Qiao, X. T., Richards, N. and Gumucio, D. L.** (2009). Dynamic patterning at the pylorus: Formation of an epithelial intestineâ "stomach boundary in late fetal life. *Developmental Dynamics* **238**, 3205–3217.
**Li, Y., Naveed, H., Kachalo, S., Xu, L. X. and Liang, J.** (2012). Mechanisms of Regulating Cell Topology in Proliferating Epithelia: Impact of Division Plane, Mechanical Forces, and Cell Memory. *PLoS ONE* **7**, e43108.
**Liu, H., Wu, Z., Shi, X., Li, W., Liu, C., Wang, D., Ye, X., Liu, L., Na, J., Cheng, H., et al.** (2013). Atypical PKC, regulated by Rho GTPases and Mek/Erk, phosphorylates Ezrin during eight-cell embryo compaction. *Developmental Biology*.
**Loomis, P. A., Kelly, A. E., Zheng, L., Changyaleket, B., Sekerková, G., Ferreira, A., Mullins, R. D. and Bartles, J. R.** (2006). Targeted wild-type and jerker espins reveal a novel, WH2-domain-dependent way to make actin bundles in cells. *J. Cell. Sci.* **119**, 1655–1665.
**Loomis, P. A., Zheng, L., Sekerková, G., Changyaleket, B., Mugnaini, E. and Bartles, J. R.** (2003). Espin cross-links cause the elongation of microvillus-type parallel actin bundles in vivo. *The Journal of Cell Biology* **163**, 1045–1055.
**Mao, Y., Hoppe, A., Kester, L., Thompson, B. J., Tournier, A. L. and Tapon, N.** (2013). Differential proliferation rates generate patterns of mechanical tension that orient tissue growth. *The EMBO Journal* **32**, 2790–2803.
**Martin, A. C. and Goldstein, B.** (2014). Apical constriction: themes and variations on a cellular mechanism driving morphogenesis. *Development* **141**, 1987–1998.
**Martin, A. C., Gelbart, M., Fernandez-Gonzalez, R., Kaschube, M. and Wieschaus, E. F.** (2010). Integration of contractile forces during tissue invagination. *The Journal of Cell Biology* **188**, 735–749.
**Martín-Belmonte, F., Gassama, A., Datta, A., Yu, W., Rescher, U., Gerke, V. and Mostov, K.** (2007). PTEN-Mediated Apical Segregation of Phosphoinositides Controls Epithelial Morphogenesis through Cdc42. *Cell* **128**, 383–397.
**Mathan, M., Moxey, P. C. and Trier, J. S.** (1976). Morphogenesis of fetal rat duodenal villi. *Am. J. Anat.* **146**, 73–92.
**Meyer, E. J., Ikmi, A. and Gibson, M. C.** (2011). Interkinetic Nuclear Migration Is a Broadly Conserved Feature of Cell Division in Pseudostratified Epithelia. *Current Biology* **21**, 485–491.
**Minc, N., Burgess, D. and Chang, F.** (2011). Influence of Cell Geometry on Division-Plane Positioning. *Cell* **144**, 414–426.
**Monier, B., Gettings, M., Gay, G., Mangeat, T., Schott, S., Guarner, A. and Suzanne, M.** (2015). Apico-basal forces exerted by apoptotic cells drive epithelium folding. *Nature* **518**, 245–248.
**Moxey, P. C. and Trier, J. S.** (1979). Development of villus absorptive cells in the human fetal small intestine: A morphological and morphometric study. *The Anatomical Record* **195**, 463–482.
**Nelson, C. M. and Gleghorn, J. P.** (2012). Sculpting Organs: Mechanical Regulation of Tissue

Development. *Annu. Rev. Biomed. Eng.* **14**, 129–154.
**Nelson, C. M., Jean, R. P., Tan, J. L., Liu, W. F., Sniadecki, N. J., Spector, A. A. and Chen, C. S.** (2005). Emergent patterns of growth controlled by multicellular form and mechanics. *Proc. Natl. Acad. Sci. U.S.A.* **102**, 11594–11599.
**Nelson, W. J.** (2003). Adaptation of core mechanisms to generate cell polarity. *Nature* **422**, 766–774.
**Nishimura, M., Inoue, Y. and Hayashi, S.** (2007). A wave of EGFR signaling determines cell alignment and intercalation in the Drosophila tracheal placode. *Development* **134**, 4273–4282.
**Nowotschin, S. and Hadjantonakis, A.-K.** (2010). Cellular dynamics in the early mouse embryo: from axis formation to gastrulation. *Current Opinion in Genetics & Development* **20**, 420–427.
**Odell, G. M., Oster, G., Alberch, P. and Burnside, B.** (1981). The mechanical basis of morphogenesis. *Developmental Biology* **85**, 446–462.
**Pinson, K. I., Dunbar, L., Samuelson, L. and Gumucio, D. L.** (1998). Targeted disruption of the mouse villin gene does not impair the morphogenesis of microvilli. *Developmental Dynamics* **211**, 109–121.
**Polyakov, O., He, B., Swan, M., Shaevitz, J. W., Kaschube, M. and Wieschaus, E.** (2014). Passive Mechanical Forces Control Cell-Shape Change during Drosophila Ventral Furrow Formation. *Biophysical Journal* **107**, 998–1010.
**Qin, Y., Meisen, W. H., Hao, Y. and Macara, I. G.** (2010). Tuba, a Cdc42 GEF, is required for polarized spindle orientation during epithelial cyst formation. *The Journal of Cell Biology* **189**, 661–669.
**Rauskolb, C., Sun, S., Sun, G., Pan, Y. and Irvine, K. D.** (2014). Cytoskeletal tension inhibits Hippo signaling through an Ajuba-Warts complex. *Cell* **158**, 143–156.
**Revenu, C., Ubelmann, F., Hurbain, I., Marjou, El, F., Dingli, F., Loew, D., Delacour, D., Gilet, J., Brot-Laroche, E., Rivero, F., et al.** (2012). A new role for the architecture of microvillar actin bundles in apical retention of membrane proteins. *Molecular Biology of the Cell* **23**, 324–336.
**Rodriguez-Boulan, E. and Macara, I. G.** (2014). Organization and execution of the epithelial polarity programme. *Nat Rev Mol Cell Biol* **15**, 225–242.
**Rodríguez-Fraticelli, A. E., Gálvez-Santisteban, M. and Martín-Belmonte, F.** (2011). Divide and polarize: recent advances in the molecular mechanism regulating epithelial tubulogenesis. *Current Opinion in Cell Biology* **23**, 638–646.
**Röper, K.** (2015). Chapter Four-Integration of Cell–Cell Adhesion and Contractile Actomyosin Activity During Morphogenesis. *Current topics in developmental biology* **112**, 103–127.
**Ruemmele, F. M., Müller, T., Schiefermeier, N., Ebner, H. L., Lechner, S., Pfaller, K., Thöni, C. E., Goulet, O., Lacaille, F., Schmitz, J., et al.** (2010). Loss-of-function of MYO5B is the main cause of microvillus inclusion disease: 15 novel mutations and a CaCo-2 RNAi cell model. *Hum. Mutat.* **31**, 544–551.
**Saotome, I., Curto, M. and McClatchey, A. I.** (2004). Ezrin is essential for epithelial organization and villus morphogenesis in the developing intestine. *Developmental Cell* **6**, 855–864.
**Sauvanet, C., Wayt, J., Pelaseyed, T. and Bretscher, A.** (2015). Structure, Regulation, and Functional Diversity of Microvilli on the Apical Domain of Epithelial Cells. *Annu. Rev. Cell Dev. Biol.* **31**, 593–621.

**Schlüter, M. A., Pfarr, C. S., Pieczynski, J., Whiteman, E. L., Hurd, T. W., Fan, S., Liu, C.-J. and Margolis, B.** (2009). Trafficking of Crumbs3 during cytokinesis is crucial for lumen formation. *Molecular Biology of the Cell* **20**, 4652–4663.

**Shyer, A. E., Huycke, T. R., Lee, C., Mahadevan, L. and Tabin, C. J.** (2015). Bending Gradients: How the Intestinal Stem Cell Gets Its Home. *Cell* **161**, 569–580.

**Shyer, A. E., Tallinen, T., Nerurkar, N. L., Wei, Z., Gil, E. S., Kaplan, D. L., Tabin, C. J. and Mahadevan, L.** (2013). Villification: How the Gut Gets Its Villi. *Science* **342**, 212–218.

**Spence, J. R., Lauf, R. and Shroyer, N. F.** (2011). Vertebrate intestinal endoderm development. *Developmental Dynamics* **240**, 501–520.

**Stelzner, M. and Chen, D. C.** (2006). To Make a New Intestinal Mucosa. *Rejuvenation Research* **9**, 20–25.

**Takeichi, M.** (2014). Dynamic contacts: rearranging adherens junctions to drive epithelial remodelling. *Nat Rev Mol Cell Biol* **15**, 397–410.

**Taniguchi, K., Shao, Y., Townshend, R. F., Tsai, Y.-H., DeLong, C. J., Lopez, S. A., Gayen, S., Freddo, A. M., Chue, D. J., Thomas, D. J., et al.** (2015). Lumen Formation Is an Intrinsic Property of Isolated Human Pluripotent Stem Cells. *Stem Cell Reports* **5**, 954–962.

**Tawk, M., Araya, C., Lyons, D. A., Reugels, A. M., Girdler, G. C., Bayley, P. R., Hyde, D. R., Tada, M. and Clarke, J. D. W.** (2007). A mirror-symmetric cell division that orchestrates neuroepithelial morphogenesis. *Nature* **446**, 797–800.

**Tepass, U.** (2012). The Apical Polarity Protein Network in DrosophilaEpithelial Cells: Regulation of Polarity, Junctions, Morphogenesis, Cell Growth, and Survival. *Annu. Rev. Cell Dev. Biol.* **28**, 655–685.

**Trumbo, P., Schlicker, S., Yates, A. A., Poos, M.Food and Nutrition Board of the Institute of Medicine, The National Academies** (2002). Dietary reference intakes for energy, carbohydrate, fiber, fat, fatty acids, cholesterol, protein and amino acids. *J Am Diet Assoc* **102**, 1621–1630.

**Villasenor, A., Chong, D. C., Henkemeyer, M. and Cleaver, O.** (2010). Epithelial dynamics of pancreatic branching morphogenesis. *Development* **137**, 4295–4305.

**Viotti, M., Nowotschin, S. and Hadjantonakis, A.-K.** (2014). SOX17 links gut endoderm morphogenesis and germ layer segregation. *Nature Cell Biology* **16**, 1146–1156.

**Walker-Smith, J. A., Guandalini, S., Schmitz, J., Shmerling, D. H. and Visakorpi, J. K.** (1990). Revised criteria for diagnosis of coeliac disease. Report of Working Group of European Society of Paediatric Gastroenterology and Nutrition. *Archives of Disease in Childhood* **65**, 909.

**Walton, K. D., Kolterud, A., Czerwinski, M. J., Bell, M. J., Prakash, A., Kushwaha, J., Grosse, A. S., Schnell, S. and Gumucio, D. L.** (2012). Hedgehog-responsive mesenchymal clusters direct patterning and emergence of intestinal villi. *Proc. Natl. Acad. Sci. U.S.A.* **109**, 15817–15822.

**Walton, K. D., Whidden, M., Kolterud, A., Shoffner, S. K., Czerwinski, M. J., Kushwaha, J., Parmar, N., Chandhrasekhar, D., Freddo, A. M., Schnell, S., et al.** (2016). Villification in the mouse: Bmp signals control intestinal villus patterning. *Development* **143**, 427–436.

**Weale, A. R., Edwards, A. G. and Bailey, M.** (2005). Intestinal adaptation after massive intestinal resection. *Postgraduate medical …*.

**Whiteman, E. L., Fan, S., Harder, J. L., Walton, K. D., Liu, C.-J., Soofi, A., Fogg, V. C., Hershenson, M. B., Dressler, G. R., Deutsch, G. H., et al.** (2014). Crumbs3 Is Essential

for Proper Epithelial Development and Viability. *Molecular and Cellular Biology* **34**, 43–56.
**Wiegerinck, C. L., Janecke, A. R., Schneeberger, K., Vogel, G. F., van Haaften Visser, D. Y., Escher, J. C., Adam, R., Thöni, C. E., Pfaller, K., Jordan, A. J., et al.** (2014). Loss of Syntaxin 3 Causes Variant Microvillus Inclusion Disease. *Gastroenterology* **147**, 65–68.e10.
**Yamaguchi, Y. and Miura, M.** (2012). How to form and close the brain: insight into the mechanism of cranial neural tube closure in mammals. *Cell. Mol. Life Sci.* **70**, 3171–3186.
**Yamaguchi, Y., Shinotsuka, N., Nonomura, K., Takemoto, K., Kuida, K., Yosida, H. and Miura, M.** (2011). Live imaging of apoptosis in a novel transgenic mouse highlights its role in neural tube closure. *The Journal of Cell Biology* **195**, 1047–1060.
**Yonemura, S., Wada, Y., Watanabe, T., Nagafuchi, A. and Shibata, M.** (2010). α-Catenin as a tension transducer that induces adherens junction development. *Nature Cell Biology* **12**, 533–542.
**Yu, S., Nie, Y., Knowles, B., Sakamori, R., Stypulkowski, E., Patel, C., Das, S., Douard, V., Ferraris, R. P., Bonder, E. M., et al.** (2014). TLR sorting by Rab11 endosomes maintains intestinal epithelial-microbial homeostasis. *The EMBO Journal* **33**, 1882–1895.
**Zheng, L., Sekerková, G., Vranich, K., Tilney, L. G., Mugnaini, E. and Bartles, J. R.** (2000). The Deaf Jerker Mouse Has a Mutation in the Gene Encoding the Espin Actin-Bundling Proteins of Hair Cell Stereocilia and Lacks Espins. *Cell* **102**, 377–385.
**Zheng, Z., Zhu, H., Wan, Q., Liu, J., Xiao, Z., Siderovski, D. P. and Du, Q.** (2010). LGN regulates mitotic spindle orientation during epithelial morphogenesis. *The Journal of Cell Biology* **189**, 275–288.
**Zieve, G. W., Turnbull, D., Mullins, J. M. and McIntosh, J. R.** (1980). Production of large numbers of mitotic mammalian cells by use of the reversible microtubule inhibitor nocodazole. Nocodazole accumulated mitotic cells. *Experimental Cell Research* **126**, 397–405.
**Zlotek-Zlotkiewicz, E., Monnier, S., Cappello, G., Le Berre, M. and Piel, M.** (2015). Optical volume and mass measurements show that mammalian cells swell during mitosis. *The Journal of Cell Biology* **211**, 765–774.

# Chapter II

# Coordination of signaling and tissue mechanics during morphogenesis of murine intestinal villi: A role for mitotic cell rounding*

**Abstract**

The main function of the small intestine is to digest and absorb nutrients; efficient function requires a very large surface area, which in part is ensured by the presence of villi, fingerlike epithelial projections that extend into the lumen. Prior to villus formation, the epithelium is a thick pseudostratified layer. In mice, beginning at embryonic day (E)14.5, mesenchymal cell clusters form just beneath the thick epithelium. Analysis of the lumenal surface at this time reveals a regular pattern of short apical membrane invaginations that form in regions of the epithelium that lie between mesenchymal clusters. Invaginations begin in the proximal intestine and spread distally, deepening with time. Interestingly, mitotically rounded cells are frequently associated with invaginations. These mitotic cells are located at the tips of the invaginating

* Note this chapter represents the following manuscript submitted for publication

**Freddo AM, Shoffner SK, Shao Y, Taniguchi K, Grosse AS, Guysinger MN, Wang S, Rudraraju S, Margolis B, Garikipati K, Schnell S, Gumucio DL.** (2016) Coordination of signaling and tissue mechanics during morphogenesis of murine intestinal villi: A role for mitotic cell rounding. *Integrative Biology*, Submitted.

membrane, rather than at the apical surface. Further investigation of epithelial changes during membrane invagination reveals that epithelial cells above each cluster shorten and widen. As a result, epithelial cells located between clusters experience a compressive force from the expansion of the surrounding cells. Using a computational model, we examined whether such forces are sufficient to cause apical invaginations. Simulations reveal that proper apical membrane invagination requires both intraepithelial compressive forces and mitotic cell rounding in the compressed regions. Together, these data establish a new model that explains how signaling events intersect with tissue forces to pattern apical membrane invaginations that define the villus boundaries.

**Introduction**

The intestine requires an enormous surface area for effective nutrient absorption. Multiple morphological adaptations contribute to this large absorptive surface, including the remarkable length of the intestine (2-4 meters in humans) (Helander and Fändriks, 2014), convolution of its mucosa into fingerlike projections known as villi (Madara, 2010; Mathan et al., 1976; Moxey and Trier, 1979), and the presence of thousands of microvilli on the apical surface of each epithelial cell (Sauvanet et al., 2015). Factors that severely reduce intestinal absorptive surface, whether due to congenital (e.g., short bowel syndrome, microvillus atrophy) or traumatic (e.g., necrotizing enterocolitis, volvulus) etiologies can result in intestinal failure, a life-threatening condition for which there are few treatment options (Goulet and Ruemmele, 2006; Goulet et al., 2004; Stelzner and Chen, 2006).

The presence of villi has been estimated to provide a 6.5-fold amplification of intestinal surface area in humans (Helander and Fändriks, 2014). Interestingly, the number of villi appears

to be largely established by the time of birth; in rodent models of intestinal resection, adaptation consists largely of growth in villus length and girth with little increase in villus number (Clarke, 1967; Forrester, 1972; Helmrath et al., 1996). Thus, the active generation of villi that occurs in fetal life provides the best opportunity for investigation of the morphogenic and molecular pathways required for villus formation.

In mice, the first intestinal villi emerge at embryonic day (E)14.5. At this time, the epithelium is over 50 μm thick with nuclei located at staggered positions, which led early investigators to conclude that the epithelium is stratified (Madara, 2010; Mathan et al., 1976; Toyota et al., 1989). Furthermore, it was thought that villus domains are established via changes in epithelial cell polarity that result in the formation of *de novo* secondary lumens between cell layers and subsequent fusion of these isolated lumens with the primary lumen (Mathan et al., 1976). These long-held notions of villus morphogenesis have recently been dispelled; new evidence from 3D imaging studies reveals a single-layered pseudostratified epithelium with no evidence for disconnected secondary lumens (Grosse et al., 2011).

It is well established that villus formation involves signaling cross-talk between the intestinal epithelium and the underlying mesenchyme (Grosse et al., 2011; Karlsson et al., 2000; Kolterud et al., 2009; Walton et al., 2012). One of the key signals for initiating villus formation is Hedgehog (Hh). Hh ligands secreted from the epithelium stimulate nearby mesenchymal cells to form clusters beneath and closely associated with the epithelium (Kolterud et al., 2009; Walton et al., 2012; Walton et al., 2016). These clusters form in a patterned array, beginning in the duodenum and spreading distally, towards the colon; their pattern appears to be controlled by a self-organizing Turing field that depends on Bmp signaling (Walton et al., 2016). Importantly, while Bmp signals organize the distribution of mesenchymal clusters, patterning of the villus

boundaries in the overlying epithelium is independent of Bmp signal transduction by epithelial cells (Walton et al., 2016). Therefore, additional components are required to explain how villus domains are defined in the epithelium.

It is also important to consider the speed of villus demarcation. In the mouse, it takes approximately 36 hours (from E14.5 to E16.0) for the initial wave of clusters to propagate from pylorus to cecum (Walton et al., 2012). Because the intestine is 30 mm long at E15.5, this morphogenic wave moves at a speed of over 800 μm per hour, nearly 15 μm per minute.

To begin to address the mechanisms by which the thick pseudostratified epithelium could be rapidly parsed into separate villus domains, we examined the earliest apical surface deformation in the intestinal epithelium and detected a patterned array of short apical membrane invaginations, or folds, that initiate proximally and spread distally, deepening with time. These folds, which represent the first signs of villus morphogenesis, form predominantly in regions of the epithelium that are not in direct contact with the pre-existing mesenchymal clusters.

Further investigation of these initial apical deformations reveals that they are frequently associated with the presence of rounded mitotic cells, suggesting a relationship between cell division and villus morphogenesis. Cell divisions play an important role in apical expansion in at least two other *in vivo* systems: the developing zebrafish neural keel, where apical polarization during cell division establishes the central lumen (Buckley et al., 2013; Tawk et al., 2007) and formation of the *Drosophila* tracheal placode, where mitotic cell rounding facilitates rapid invagination of epithelial regions that are under passive circumferential compression (Kondo and Hayashi, 2013; Nishimura et al., 2007). We therefore tested whether either of these two models could explain the invaginations associated with villus morphogenesis in the developing intestinal epithelium.

We show here that the process of villus morphogenesis closely resembles tracheal placode invagination from morphological, temporal, and mechanical perspectives. We identify epithelial cell shape changes adjacent to mesenchymal clusters that can exert patterned intraepithelial pressure to initiate apical invaginations. We further demonstrate a robust association between apical invaginations and mitotic cells; these cells undergo "internalized cell rounding," a process by which mitosis-associated cell rounding is accompanied by rapid depression of the apical surface (Kondo and Hayashi, 2013). These *in vivo* observations were used to develop a computational model that allowed further exploration of the mechanical forces required for apical invagination.

These data suggest a new model for villus morphogenesis in which signaling events, initiated by a regular array of mesenchymal clusters, produce a pattern of intraepithelial mechanical forces that, when triggered by mitotic cells, promote rapid apical invaginations. This model establishes a mechanism by which a mesenchymal pattern can be rapidly transferred to the epithelium to establish villus boundaries.

## Results

### *Apical expansion during villus morphogenesis*

We previously documented that villus morphogenesis involves expansion of the main lumen rather than formation and fusion of disconnected secondary lumens (Grosse et al., 2011). To further explore the initial changes in the apical surface that accompany this expansion, we examined this process in E13.5 to E15.5 intestines utilizing antibodies to EZRIN, an apical surface protein (Fehon et al., 2010), and PDGFRα, a marker of the mesenchymal clusters

involved in villus patterning (Walton et al., 2012). Both cross sections (Figure II-1A-C) and longitudinal sections (Figure II-1D-F) of tissue were examined.

At E13.5, the epithelium is uniformly pseudostratified and the apical surface is flat; mesenchymal clusters are not detectable (Figure II-1A and D). At E14.5, mesenchymal clusters are visible in the proximal, but not distal intestine. Clusters are tightly associated with the overlying epithelium, sitting in small alcoves and slightly deforming the basal surface of the pseudostratified epithelium (Figure II-1B and E, asterisks). The apical surface, however, remains flat, with occasional short extensions of EZRIN staining oriented perpendicularly to the lumenal surface in the proximal intestine (Figure II-1B and E, arrows). By E15.5, these apical extensions are deeper and a field of regularly patterned villi cover the proximal intestine, such that each villus is closely associated with a mesenchymal cluster (Figure II-1C and F). All of these events first occur in the proximal intestine and after about one day are present distally, consistent with previous findings that villus formation occurs in a proximal to distal wave (Mathan et al., 1976; Walton et al., 2012).

*Spatiotemporal characterization of apical lumen expansion*

The spatial patterning of EZRIN positive apical extensions was then examined. These experiments were performed using an intestinal explant culture; in such explants, the rate of villus morphogenesis slows, allowing greater resolution of the morphogenic process (Walton et al., 2012). The location of apical extensions relative to mesenchymal clusters was quantified. In the proximal E14.5 and distal E15.5 intestine, where the morphogenic front of villus emergence is located, over 80% of the apical deformations were found in epithelial regions that lie between rather than over clusters (Figure II-1G).

A spatiotemporal correlation was also apparent between the depth of apical extensions and their location along the proximal-distal axis: at E15.0, midway through the morphogenic process, these indentations are deeper in the proximal compared with distal regions of the same intestine (Figure II-1H). This mirrors the established pattern of cluster formation, as clusters first form in the proximal duodenum and spread in a wave-like fashion down the intestine over a 36 hour period (E14.5 to E16.0) (Walton et al., 2012). Because clusters are known to mark the core of villus domains (Walton et al., 2012), these short apical extensions appear to represent the initial boundaries between villi.

*Three-dimensional visualization of apical surface changes*

To better understand the three-dimensional structure and pattern of apical surface extensions during initial villus demarcation, two approaches were taken. First, thick (100 μm) vibratome sections were stained with phalloidin to mark the apical F-actin network. Confocal Z stacks were generated and reconstructed in three dimensions to determine the shape of individual extensions (Figure II-2A-B). These studies establish that the smallest extensions consist of closely opposed double-membrane folds or invaginations, with little lumenal space between membranes. Importantly, as these folds deepen, they remain continuous with the apical surface. Previous work has established that the apical surface remains continuous throughout villus development (Grosse et al., 2011).

To further appreciate the patterning of these invaginations, intestines from embryos ranging from E14.0 to E14.5 were longitudinally opened and scanning electron microscopy (SEM) was used to image the apical surface. In E14.0 intestines, the surface is flat, though cellular outlines are visible (Figure II-2C). Beginning in the duodenum at E14.5, a dramatic

transition can be observed along the proximal to distal axis; domes surrounded by deep creases are located more proximally to areas of disconnected invaginations (Figure II-2D). The field seen in this image, which appears to represent the transitional front of the morphogenic wave, measures slightly more than 150 μm. Assuming that this wave moves at a constant speed between E14.5 and E15.5 (Walton et al., 2012), we calculate that the transition seen in Figure II-2D should take place in about 10 minutes.

*Patterned apoptosis does not explain fold distribution*

The data above indicate that apical invaginations appear beginning at E14.5 in a spatiotemporally controlled pattern in the developing intestine and that these invaginations are likely nascent villus demarcations. We next sought a mechanism to explain the appearance of these invaginations. During morphogenesis of the *Drosophila* leg, apoptosis facilitates epithelial folding by coupling cell death to the transmission of physical forces (Monier et al., 2015). Additionally, in the early neural ectoderm, apoptosis generates force to assist tissue bending before neural tube closure (Yamaguchi and Miura, 2012; Yamaguchi et al., 2011). To determine whether localized apoptosis might cause apical folding during villus morphogenesis, we examined the pattern of cleaved Caspase 3 staining in E14.5 intestines. This analysis revealed that the frequency of apoptosis is very low both before and during villus morphogenesis (Figure II-3). The rare apoptotic figures scattered throughout the epithelium do not appear to correspond with apical surface extensions or mesenchymal clusters. Therefore, the establishment of villus domains is not determined by localized patterns of apoptosis.

*Apical folds are associated with dividing cells*

Another event that has been associated with the generation of new apical surfaces is mitosis (Buckley et al., 2013; Kondo and Hayashi, 2013; Schlüter et al., 2009; Taniguchi et al., 2015; Tawk et al., 2007; Wang et al., 2014). We therefore examined the distribution of dividing epithelial cells during the process of apical expansion. Interestingly, 40% of pHH3+ mitotic figures were found at the tips of invaginations (Figure II-4A-B). This association is remarkable considering that the tips of these folds constitute a small proportion of the total apical surface (Figure II-4A). Moreover, approximately 60% of folds have an associated cell division (Figure II-4C).

Because these data suggest a potential mechanistic link between mitotic cells and membrane invaginations, we examined two methods by which mitotic cells promote apical expansion in other systems. First, a new lumenal surface can form *de novo* between daughter cells during cell division; this happens in the zebrafish neural keel (Buckley et al., 2013; Tawk et al., 2007), in the formation of bile canaliculi *in vitro* and *in vivo* (Wang et al., 2014), and in isolated epithelial cells plated in a thick 3D matrix (Schlüter et al., 2009; Taniguchi et al., 2015). Alternatively, cell division can accelerate the process of apical invagination, as in the *Drosophila* tracheal placode (Kondo and Hayashi, 2013).

*Dividing cells at folds are not enriched for apical components*

Within the zebrafish neural keel or in MDCK cells plated in a 3D matrix, a unique lumen-forming cell division occurs. In these divisions, intracellular collections of apical components such as CRB3 and Pard3 are observed at the two poles of the dividing cells. During cytokinesis, these components traffic along the mitotic spindle to initiate lumen formation

between daughter pronuclei (Buckley et al., 2013; Schlüter et al., 2009; Tawk et al., 2007). To examine CRB3 distribution during cell division in the intestinal epithelium, we studied its localization in sections co-stained with α-TUBULIN (Figure II-5). No intracellular staining was found in the 30 divisions examined. Though not definitive, these data suggest that the mitotic cells at apical invaginations are not likely to be generating apical surfaces *de novo*. Thus, we explored whether mitosis-associated invagination could provide an explanation for lumenal expansion, as in the *Drosophila* tracheal placode.

*Apical intestinal invagination resembles* Drosophila *tracheal placode invagination*

Prior to invagination in the *Drosophila* tracheal placode, intercalating cells around the presumptive placode expand the surrounding epithelium, placing a passive intraepithelial compressive force on placode cells. As described by Kondo and Hayashi, as a cell within this compressed region begins mitosis, the circumferential pressure causes its apical contact to shrink and the rounded cell moves away from the apical surface while retaining a T-shaped apical extension (Supplementary Figure 8 in (Kondo and Hayashi, 2013)). This is referred to as "internalized cell rounding" and is distinct from surface cell rounding that typically characterizes mitosis in a pseudostratified epithelium. Overall, these events cause a rapid inward folding of the apical surface. The defining morphological and physical characteristics of this model include the presence of internalized mitotic cell rounding and a source of patterned intraepithelial pressure (Kondo and Hayashi, 2013; Nishimura et al., 2007).

Examination of rounded mitotic cells in the intestinal epithelium at E14.5 and E15.5 revealed two distinct morphologies. Mitotic cells that are not associated with apical invaginations round up directly adjacent to the main lumenal surface, as expected in a

pseudostratified epithelium. Some of these cells are associated with a small V-shaped indentation of the apical surface, although internalized cell rounding is not observed (Figure II-6A-B). In contrast, rounded mitotic cells associated with initial apical invaginations are positioned well below the apical surface and are connected to the main lumen by a short T-shaped apical fold that stains with apical markers such as EZRIN. The rounded cell retains a very small EZRIN-positive apical surface at the tip of the invagination (Figure II-6A, C). These cells are morphologically indistinguishable from those previously noted in the *Drosophila* tracheal placode. Such internally rounded cells cannot be detected prior to cluster formation at E14.5.

Tracheal placode invagination takes place in the context of passive compression of presumptive placode cells due to expansion of the surrounding epithelium (Kondo and Hayashi, 2013). If a similar process occurs in the intestinal epithelium, a source of compressive pressure is required. Because initial intestinal invaginations are consistently located between clusters (Figure II-1G), an attractive hypothesis is that a cluster-dependent pattern of intraepithelial compression is generated. As demonstrated above, analysis of the epithelium prior to apical invagination reveals that clusters deform the basal epithelial surface. Early investigators noted this deformation as well and suggested that clusters "push up" into the overlying epithelium (Mathan et al., 1976). However, the flat apical surface at this time argues against simple displacement of epithelial cells by the clusters. An alternative explanation is that clusters signal to overlying epithelial cells to cause them to change shape. Indeed, epithelial cells overlying clusters are up to 30% shorter than those in the inter-cluster regions at a time when minimal to no deformation is detectable at the apical surface (Figure II-7A-C).

To accommodate this basal to apical shortening, cell volume must rapidly decrease or cells must widen circumferentially. To examine these possibilities, Imaris image analysis

software was first used to compare the volume of cells over clusters and between clusters. While individual volume is quite variable, these measurements reveal a similar range of volumes in both locations (Figure II-7D), arguing against volume change as a compensation for this rapid change in cell height. Similarly, in other morphogenic systems characterized by rapid cell shape changes, cell volume is constant (Gelbart et al., 2012; Odell et al., 1981; Polyakov et al., 2014).

Because of the non-linear elastic response of the cytoplasm (Moeendarbary et al., 2013), the vertical shortening of these cells would predict a lateral increase in cell width. To determine if this effect is observed in the intestinal epithelium, the number of epithelial cells (nuclei) per unit apical length was determined in regions overlying mesenchymal clusters and in regions between clusters. These measurements revealed a lower density of nuclei per unit of apical surface in regions over clusters, suggesting that cells in this region are indeed wider (Figure II-7E). Additionally, we utilized confocal microscopy of whole-mount E15.0 intestines in which the intestine was longitudinally opened to directly image the apical surface. Reconstruction of the epithelium stained with E-cadherin to mark cell outlines revealed a clear expansion of epithelial cells directly over clusters relative to the intervening epithelial cells, which appeared more compacted (Figure II-7F). Thus, epithelial cell shape changes initiated by the presence of mesenchymal clusters could exert a patterned field of compressive forces on the intervening epithelium.

*Computational model of the mechanics of apical invagination*

To explore whether this pattern of forces could potentially explain the patterning and morphology of initial apical folds, a two-dimensional (plane strain) finite element model of the intestine was constructed using the commercial software Abaqus 6.14.1. The epithelium contains

two structural layers with differing mechanical properties: the apical layer contains the cross-linked actin-rich cytoskeleton network and the cell body layer represents the rest of the epithelium. In this model, these layers are represented by regions of different mechanical properties (Table II-1). The geometric dimensions of this model were estimated from previous experimental observations of the developing intestine. The thickness of the pre-villus epithelium has been established to be 50 μm (Grosse et al., 2011) with an apical terminal web of 1 μm (Brunser and Luft, 1970). Mesenchymal clusters are approximately 30 μm wide and 70 μm apart (Walton et al., 2012). For this reason, 15 μm is defined as a half-cluster region for each flanking region of this segment. Because mitotic cells are associated with invaginations *in vivo*, some simulations also included a rectangular region of 10 μm by 18 μm with an apical contact width of 1 μm to represent a mitotic cell. The dimensions of this model are shown in Figure II-8.

The mechanical stiffness of each region of the model was selected based on previous studies. The modulus of the actin-rich apical layer was chosen to be 10 kPa based on the measurements of the Young's modulus of actin stress fibers (Lu et al., 2008). The modulus of the cell body layer was chosen to be 0.5 kPa based on measurements of the Young's modulus of cytoplasm (Moeendarbary et al., 2013). The epithelial cytoplasm was assumed to be nearly incompressible, with Poisson's ratio of 0.495. During mitotic cell rounding, the apical actin web is disassembled, allowing the cell cortex to be stiffer than the surrounding epithelial cells such that this dividing cell can displace neighbors to accommodate rounding (Matthews et al., 2012). Therefore, the apical contact of the mitotic cell was modeled as a compliant spot with an 80% reduction in modulus compared with the rest of the apical surface.

Because the modeled region represents a repeating unit of the intestinal epithelium, symmetric boundary conditions were used for the left and right boundaries. To model the cell

shortening effects from the basal surface as observed in the *in vivo* developing epithelium, the apical surface above the clusters was constrained vertically such that the clusters would deform only the basal surface of the epithelium. Because the inter-cluster epithelium is not subject to the same signals that change cell shape over clusters, the basal inter-cluster boundary was fixed. These idealized assumptions in the model reflect hypotheses that similar conditions possibly constrain the intestinal epithelium.

To mimic the changes in cell shape that occur above mesenchymal clusters, an inelastic growth strain was applied, as is common in mechanical models of growing tissues (Garikipati, 2009; Li et al., 2011). Cell signaling leads to the shortening and widening of epithelial cells in the cluster region, which is represented by a growth strain that is positive in the lateral direction and negative in the vertical direction. To model the unchanged thickness of the apical surface during this process, only a positive lateral growth strain was applied to the apical surface above the clusters.

In initial simulations, we tested whether cluster-mediated expansion is sufficient to cause apical invaginations in the inter-cluster regions. As shown in Figure II-9A, the apical surface exhibited wave-like patterns when cluster-dependent strain was applied, but not a pronounced invagination. Because our *in vivo* observations (Figure II-4) as well as work in the *Drosophila* trachea (Kondo and Hayashi, 2013) suggest that mitotic cells might assist the invagination process, we next added a compliant defect to the apical surface, modeled as a small compliant region (yellow star in Figure II-9), to represent cytoskeletal changes during mitosis. However, no invagination was seen in these simulations (Figure II-9B), suggesting that another feature is necessary in the model.

Kondo and Hayashi report that invagination is associated with downward movement of the rounded mitotic cell into the epithelium, giving rise to internally rounded mitotic cells (Kondo and Hayashi, 2013), a feature clearly detected in the murine intestine. Therefore, additional simulations included a negative inelastic growth strain (contraction) applied in the vertical direction to both the small apical contact and the cytoplasmic region containing the cell. Combining these three features results in a fold with closely opposed membrane, similar to the T-shaped folds observed *in vivo* (Figure II-9C).

Finally, to explore whether mitosis (both the compliant apical defect and vertical contraction) is sufficient for forming invaginations, we ran simulations with these features but without cluster expansion. Interestingly, in this case, the apical surface deformed with a rounded indentation (Figure II-9D), reminiscent of the V-shaped folds observed at some dividing cells that are apically located and not associated with invaginations, and also similar in appearance to many mitotic cells before clusters form at E14.5. Together, these simulations suggest that intraepithelial forces produced by cluster-mediated epithelial shape changes and internalized mitotic cell rounding are sufficient to produce apical invaginations that mirror those seen at membrane invaginations *in vivo*.

In vivo *evidence for an apical-basal force at mitotic cells*

As shown in Figure II-6C, mitotic cells at apical intestinal folds are "internalized," a feature that they share with mitotic cells that facilitate invagination in the *Drosophila* tracheal placode. Furthermore, the computational model predicts that a contraction oriented in the apical-basal direction at the position of the mitotically rounded cell is critical for proper folding. We further explored this *in vivo* by examining E14.5 and E15.5 intestinal sections stained with

phalloidin (which marks F-actin) or phospho-myosin light chain kinase (pMLCK), markers that could reveal actin-myosin cables that might be responsible for generation of contractile forces. Staining with pMLCK reveals increased signal within dividing cells, but cable-like structures were not seen (Figure II-10A). However, enhanced actin staining was detected in the basal processes of cells dividing at invaginations (Figure II-10), potentially indicating an active downward force.

**Discussion**

The morphological events involved in villus formation were first described several decades ago. However, the use of thin sections to document the dramatic epithelial changes that occur during this process led to the incorrect conclusions that the early epithelium is stratified and that *de novo* lumen formation is an important feature of villus morphogenesis (Madara, 2010; Mathan et al., 1976; Toyota et al., 1989). The work described here utilizes recently redefined parameters regarding intestinal morphogenesis: the epithelium prior to remodeling is a single pseudostratified epithelial cell layer and lumenal expansions are invaginations of the apical surface (Grosse et al., 2011). Within this revised context, we suggest a new model to account for epithelial changes during establishment of the villus domains.

We propose that formation of the patterned invaginations that demarcate the first intestinal villi requires inputs from cell-cell signaling events combined with intraepithelial compressive forces. First, Hh signals from the thick pseudostratified epithelium cause sub-epithelial mesenchymal clusters to form (Walton et al., 2012). The positioning of these clusters is determined by a self-organizing Turing field mechanism that is driven by mesenchymal Bmp signaling (Walton et al., 2016). Over the next 36 hours, these clusters spread in a proximal to

distal wave over the length of the intestine (Walton et al., 2016; Walton et al., 2012). As they form, clusters signal to the overlying epithelium, causing these cells to change shape, shortening in the apical-basal dimension and expanding laterally. We propose that these localized shape changes over the clusters generate an intraepithelial compressive force on cells located between clusters. Within these pressurized regions, mitotic cell rounding causes rapid invagination of the apical surface.

This process of mitosis-assisted invagination is faithfully recapitulated by our computational model, demonstrating that intraepithelial mechanical forces are sufficient to result in invaginations similar to those seen *in vivo*. Three features are required to recapitulate the fold structure *in silico*: pressure from expansion of the clusters, compliancy of the apical surface at the mitotic event, and a vertical displacement of the mitotic cell in the apical-basal dimension. Removal of any of these components from the computational model results in a failure of a typical T-like invagination to occur.

Overall, the apical invagination accompanying villus morphogenesis shares many features with tracheal placode invagination in *Drosophila*. First, the process is accompanied by a patterned field of intraepithelial forces that place a passive compressive force on the regions that will indent. In the intestine, this compression likely arises from the lateral expansion of epithelial cells over clusters. Second, mitotic cells are associated with invaginations in both cases. Third, these cells have a characteristic appearance in sectioned material, previously defined as "internalized cell rounding" (Kondo and Hayashi, 2013). That is, these cells round up and enter mitosis well beneath the main surface of the epithelium, but remain connected to the lumen by the apical membrane fold. Finally, the process of invagination is very fast in both cases, taking place over a period of minutes. Live cell imaging of *Drosophila* tracheal placode invagination

shows that the initiation of mitosis in a cell within the constricted region releases the stored resistance of central cells and results in a rapid invagination (Kondo and Hayashi, 2013). In the intestine, we propose that similar forces result in the rapid demarcation of villus boundaries.

The revised model that we propose here for apical invagination in the mouse relies on the intersection of tissue mechanics with soluble signals to pattern the location of villus domains. The combined action of tissue forces and signaling is also seen during morphogenesis of the chick intestine, but the mechanistic details of that process differ significantly in chick and mouse. This might not be surprising, as it has been noted that over evolutionary time, villi likely arose independently in birds and mammals as morphological adaptations to assist nutrient absorption (Shyer et al., 2015). During "villification" in the chick, mechanical forces from the developing muscle layers pattern the eventual location of clusters and villi (Shyer et al., 2013). Formation of an inner circular smooth muscle deforms the epithelium into longitudinal ridges, and subsequent development of an outer longitudinal layer forces those ridges into zig-zags. These progressive epithelial deformations create localized maxima of Hh ligand secreted from the epithelium. Hh signals then induce the expression of mesenchymal cluster factors, such as Bmp4, which promote villus emergence from the arms of the zig-zags (Shyer et al., 2013; Shyer et al., 2015). Thus, in the chick, mechanical forces establish a pattern of epithelial deformations that then direct, via signaling, the formation of mesenchymal clusters and villi.

In contrast, in the mouse and human, formation of muscle layers does not coincide with villus formation (Lacroix et al., 1984; Matsumoto et al., 2002; Walton et al., 2016). Additionally, in mammalian species studied to date (mouse, rat, pig, and human), the epithelium never forms zig-zags, though in some cases, a few longitudinal pre-villus ridges are observed (Dekaney et al., 1997; Lacroix et al., 1984; Matsumoto et al., 2002; Nakamura and Komuro, 1983). Thus,

mechanical forces likely do not determine the patterning of mesenchymal clusters in any of these species. Rather, as demonstrated here in the mouse, a patterned field of mesenchymal clusters forms prior to any epithelial deformation. These clusters signal to overlying epithelial cells to promote cell shape changes, creating a pattern of intraepithelial forces that determine where villus boundaries will lie.

It is also noteworthy that by the time villi initiate in the chick, epithelial cells have already adopted a short columnar structure (Burgess, 1975; Shyer et al., 2013). Indeed, this flexible structure is probably required for effective muscular deformation of the epithelium that is needed to create the deep alcoves that can trap Hh signals (Shyer et al., 2013; Shyer et al., 2015). In contrast, mouse villi arise directly from a 50 μm thick pseudostratified epithelium. Thus, villus development in the mouse requires a mechanism to quickly fold this thick epithelium in a patterned manner that corresponds with the established pattern of mesenchymal clusters. We propose that the use of mitosis-associated epithelial folding can facilitate this rapid transition to generate initial villus domains.

## Materials and Methods

### Mice

All protocols for mouse experiments were approved by the University of Michigan UCUCA. C57BL/6 mice were obtained from Charles River (strain 027).

### Intestinal Explant Culture

As described previously (Walton and Kolterud, 2014; Walton et al., 2012), intestines were harvested between E13.5 and E14.5 and dissected in cold DPBS (Sigma D8537). Culturing was

performed utilizing transwells (Costar 3428) as a scaffold. BGJb media (Invitrogen 12591-038) containing 1% penicillin-streptomycin (vol/vol) (Invitrogen 15140-122) and 0.1 mg/mL ascorbic acid was placed into contact with the transwell membrane. Intestines were cultured for up to 24 hours at 37$^{o}$C with 5% $CO_2$.

Antibodies, Plasmids, and Reagents

Antibodies used were rabbit anti-aPKC 1:250 (Santa Cruz sc-216), mouse anti-α-tubulin 1:1000 (Sigma T6199), mouse anti-β-catenin 1:500 (Sigma C-7207), rabbit anti-cleaved caspase 3 1:150 (Cell Signaling 9664), rabbit anti-Crumbs3 1:250 (gift of Dr. Ben Margolis), mouse anti-E-cadherin 1:1000 (Invitrogen 13-1900), mouse anti-Ezrin 1:1500 (Sigma E8897), rabbit anti-Ki67 1:500 (Novocastra NCL-Ki67p), rabbit anti-pMLCK 1:200 (Cell Signaling 3674), rabbit anti-PDGFRα 1:200 (Santa Cruz sc-338), mouse anti-pHH3 1:1000 (Millipore 05-806), rabbit anti-pHH3 1:1000 (Millipore 06-570). Secondary antibodies used were Alexa Fluor 488/555/647-conjugated anti-mouse and anti-rabbit and Alexa Fluor 568 Phalloidin (Life Technologies A34055).

Tissue Immunofluorescence

After fixing overnight in 4% paraformaldehyde in PBS at 4$^{o}$C, intestines were washed in PBS, embedded in paraffin, and sectioned at 5 μm. Samples were deparaffinized and 10 mM sodium citrate used for antigen retrieval. Primary antibody incubation was performed overnight at 4$^{o}$C, followed by secondary antibody for 30 minutes at room temperature. Samples were imaged on a Nikon E800 (20x objective) and a Nikon A1 Confocal (20x objective, water; 60x objective, oil). Adobe Photoshop was used for image processing.

Vibratome Sectioning and Immunofluorescence

After fixation, intestines were embedded in 7% (wt/vol) low-melting agarose (Sigma A9414) in PBS and sectioned at 100 μm. Primary antibody incubation was performed overnight at 4$^{o}$C, followed by secondary antibody incubation for two hours at room temperature. Samples were mounted in Prolong Gold (Life Technologies P36930) and imaged on a Nikon A1 Confocal (20x objective, water). Image processing was done using Imaris 8.0.

Scanning Electron Microscopy

After harvest, intestines were fixed at 4$^{o}$C in 2.5% gluteraldehyde overnight and washed in Sorenson's phosphate buffer (0.1 M, pH 7.4). Overnight treatment with hexamethyldisilazane was followed by mounting and sputter coating with gold. An Amray 1910 FE Scanning Electron Microscope was used to examine samples, with images taken using Semicaps 2000 software. Image processing was done using Adobe Photoshop.

Computational Model

Modeling was done using the finite element method (FEM), which is a mesh based discretization technique for solving partial differential equations (Hughes, 2012). The computational results in this paper were generated using the FEM package Abaqus (version 6.14.1), which was used to solve the equations governing the mechanical deformation of the epithelium. The pre-villus epithelium was modeled as a 2D geometry (Figure II-8) and we assumed a hyper-elastic Holzapfel-Gasser-Ogden material model with spatially varying material properties (Table II-1).

Statistical Analysis

All graphs were made and statistical analyses performed using Prism 6. Statistical tests were used as indicated in the figure legends.

**Acknowledgments**

The authors would like to thank the University of Michigan Microscopy and Image Analysis Laboratory for assistance with preparing and imaging samples. We also would like to thank Drs. Linda Samuelson, Jason Spence, Daniel Teitelbaum, Kristen Verhey, Katherine Walton, and Yukiko Yamashita for discussions. Support was provided by NIH F30 DK100125 and the University of Michigan Medical Scientist Training Program (AMF) and NIH R01 DK089933 (DLG).

**Author Contributions**

Contributed to concepts, approaches: AMF, SKS, YS, KT, ASG, SR, KG, SS, BM, DLG

Performed experiments: AMF, MNG, SW

Performed computations: SKS, YS, SR

Analyzed data: AMF, SKS, SR, KG, SS, DLG

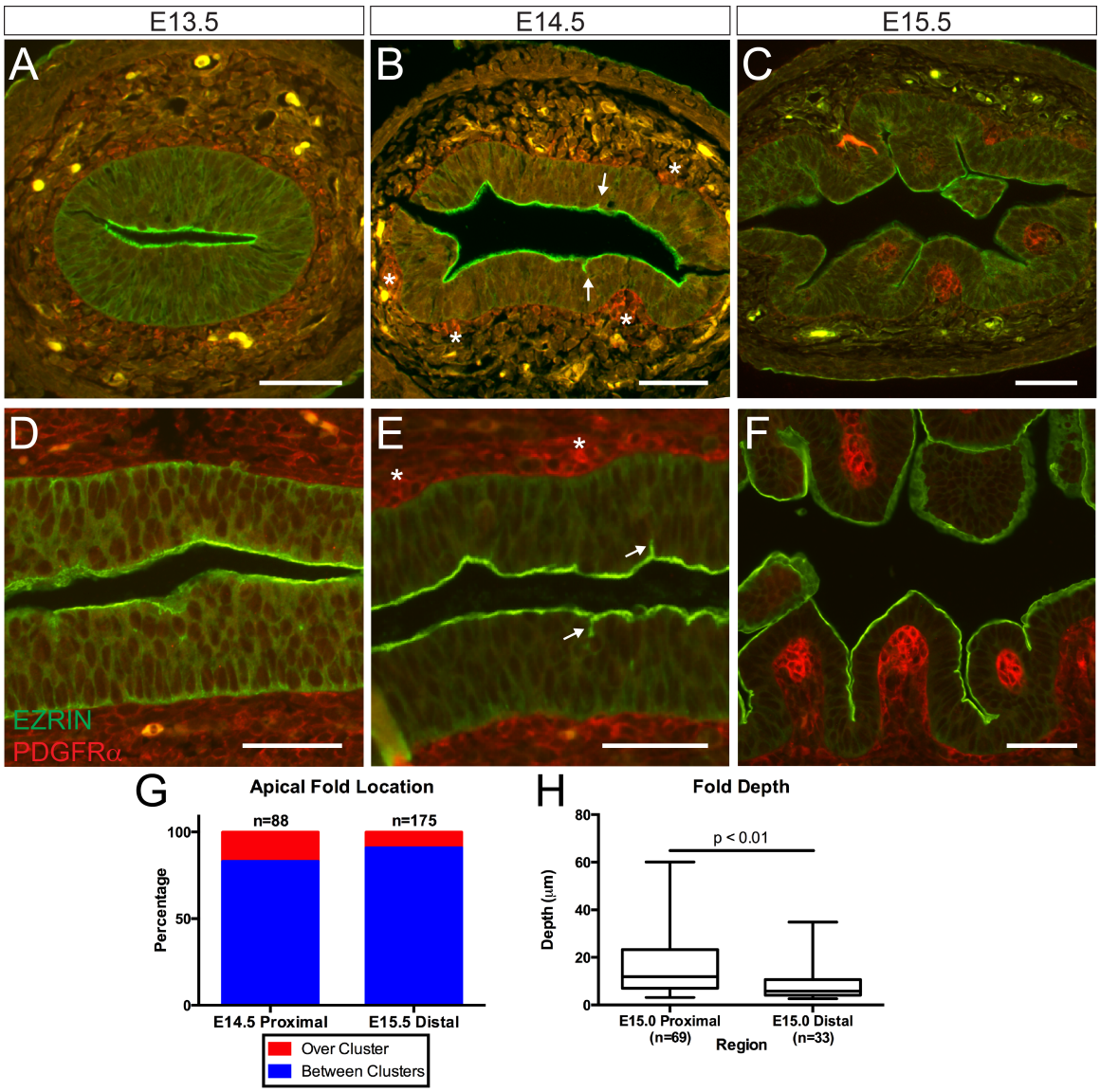


**Figure II-1. Temporal analysis of the intestinal apical surface during villus initiation.** (A-C) Cross-sections and (D-F) longitudinal sections of the murine small intestine at (A, D) E13.5, (B, E) E14.5, and (C, F) E15.5 stained with EZRIN (green) and PDGFRα (red). Initial deformations appear at E14.5 (B and E, arrows). Mesenchymal clusters are marked with asterisks. Folds deepen to clearly demarcate villi by E15.5. Scale bar = 50 μm. (G) Quantification of fold location relative to mesenchymal clusters at the morphogenic front of villus development at E14.5 and E15.5. (H) Box and whisker plots comparing fold depth in the E15.0 proximal and distal intestines showing the maximum, minimum, and median of the data sets ($p = 0.0026$, unpaired t-test).

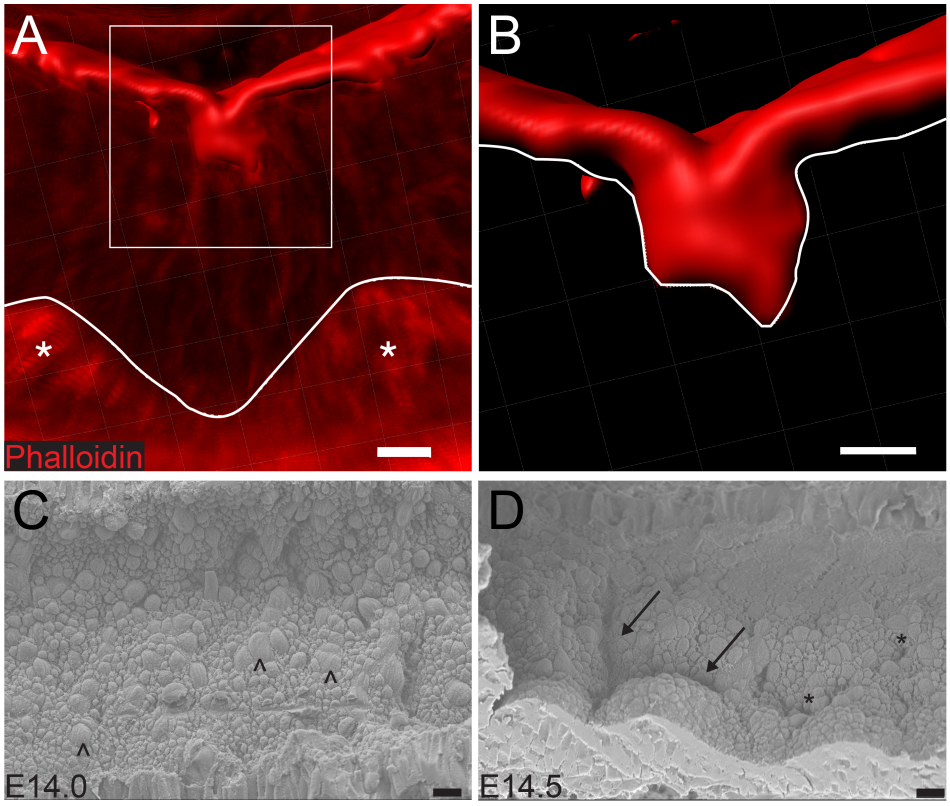


**Figure II-2. Three-dimensional analysis of apical invaginations.** (A) Reconstruction of the apical surface (phalloidin, red) indicating an early fold located between two clusters (asterisks). Images were obtained by confocal scanning of a 100 μm thick vibratome section of the E14.5 intestine, and the 3D view was reconstructed using Imaris. The basement membrane is traced with a white line. (B) Inset of box in (A), the underside of the apical surface is traced with a white line. The fold represents an invagination of the apical surface; two membrane faces are visible. Scale bar = 10 μm. (C, D) Scanning electron micrographs of the apical surface at E14.0 and E14.5. In both images, proximal is on the left and distal is on the right. (C) At E14.0, although cell boundaries are visible, the overall surface is flat. Occasional larger cell profiles represent mitotic cells (arrowheads). (D) At E14.5, deeper folds (arrows) clearly outline nascent villi. Nearby, shallower, disconnected invaginations (asterisks) are visible. Because the rate of cluster spread is 30 mm over 36 hours, or 15 μm per minute (Walton et al., 2012), the morphogenic wave can travel this 150 μm field in approximately 10 minutes. Scale bar = 10 μm.

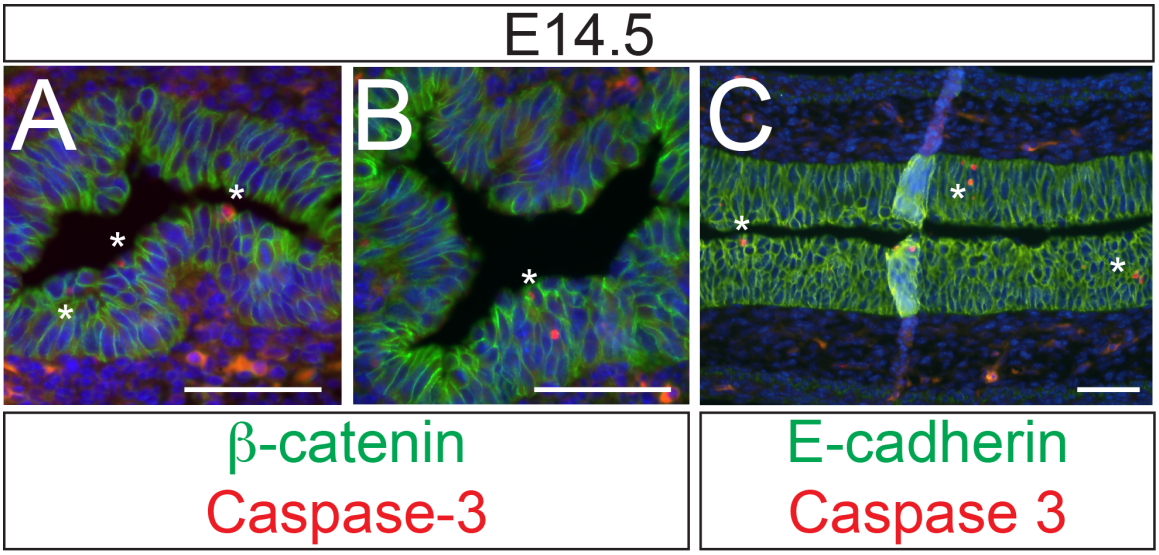


**Figure II-3. Apoptosis is infrequent in the early intestine.** (A, B) Cross-sections of the intestine at E14.5, demonstrating rare apoptotic events (asterisks, Caspase-3, red) in the epithelium containing nascent villi (β-catenin, green). (C) Longitudinal section at the same time, showing the rarity of apoptosis in the epithelium (E-cadherin, green). Scale bar = 50 μm.

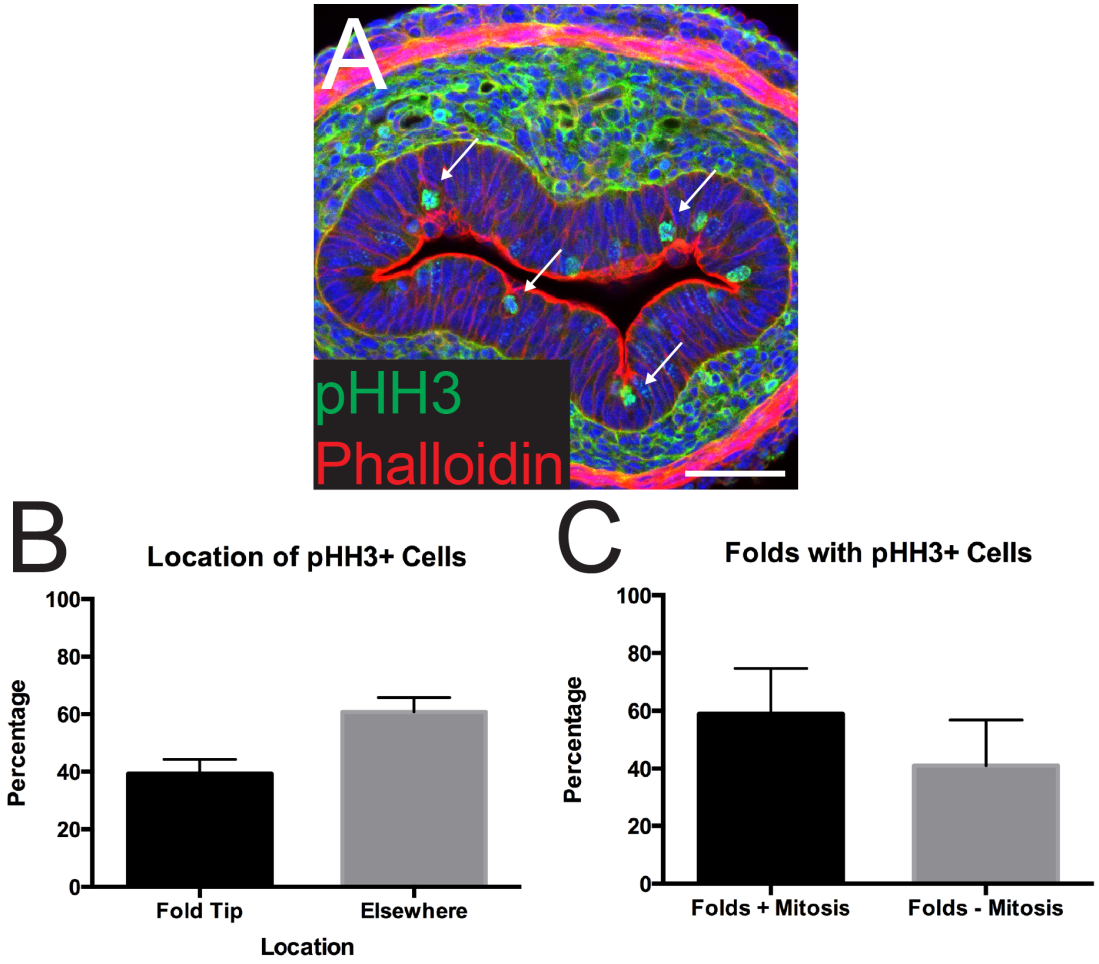


**Figure II-4. Apical folds are associated with dividing cells.** (A) Cross-section of the intestine stained with pHH3 (green) and phalloidin (red). Many apical folds are associated with mitotic cells (arrows). Note that phalloidin also stains the outer smooth muscle layer and there is some background from antibody trapping in the mesenchymal connective tissue. Scale bar = 50 μm. (B) Quantification of the location of dividing (pHH3+) cells in the epithelium at E14.5. Forty percent of invaginations are associated with a dividing cell. (C) Quantification of the number of folds associated with a dividing cell. Sixty percent of folds are associated with a cell division event. Error bars represent standard deviation.

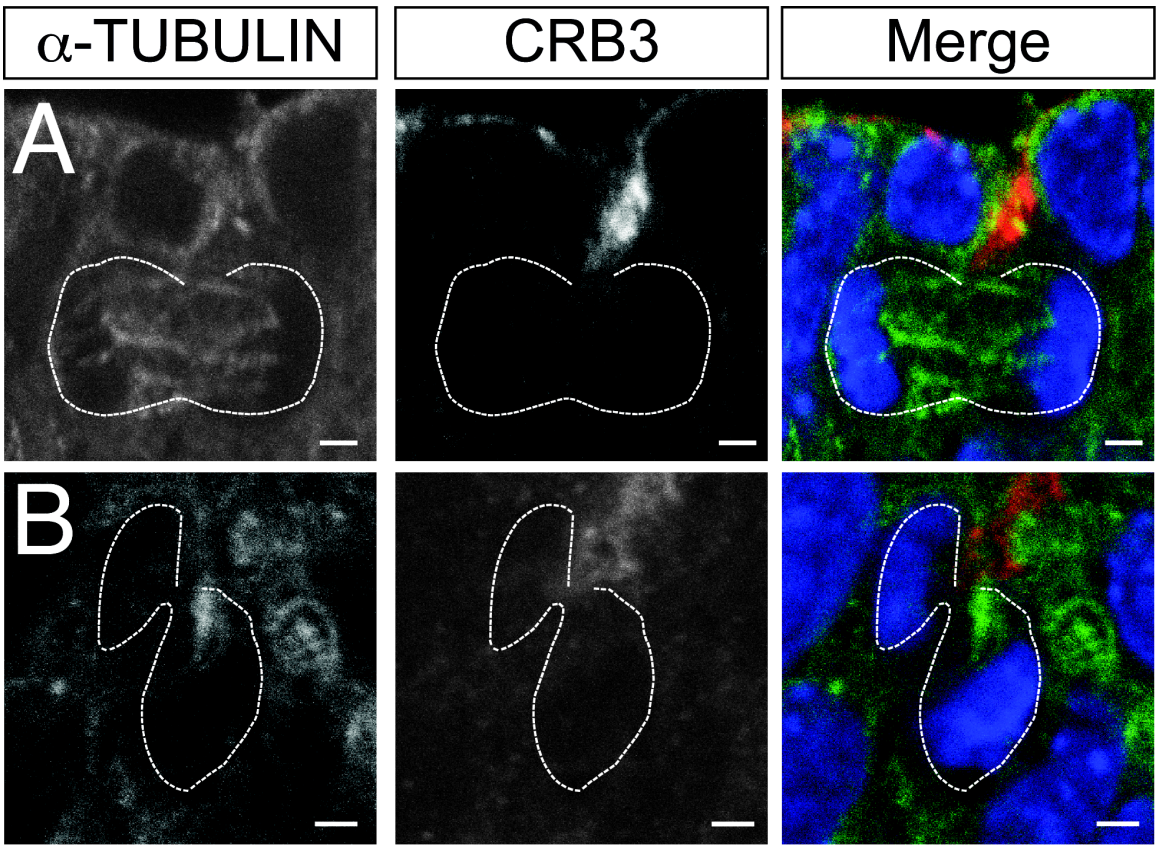


**Figure II-5. Dividing cells at fold tips do not exhibit internalized CRB3.** Two examples of dividing cells (outlined) at tips of apical folds, stained for antibodies against CRB3 (red) in (A) anaphase and apparent. Scale bar = 2 μm.

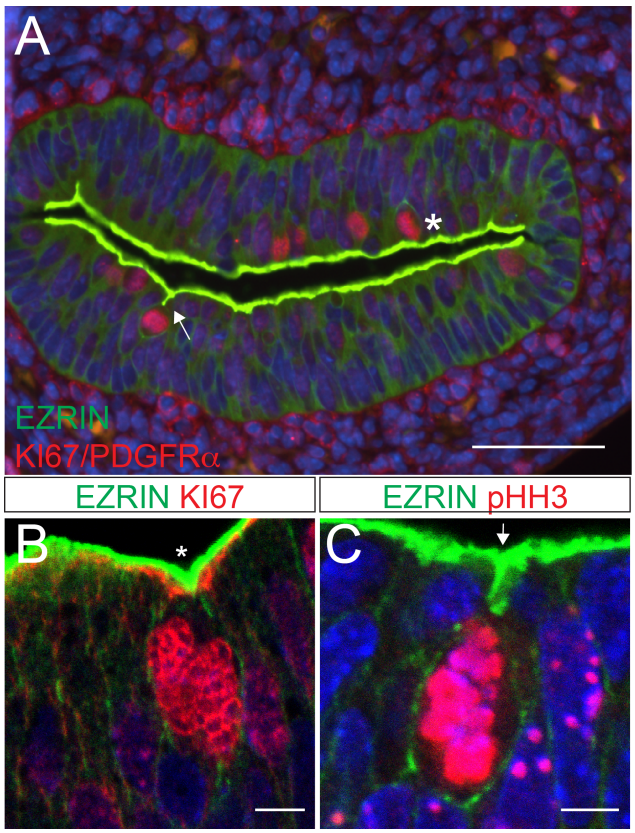


**Figure II-6. Two types of cell division in the intestinal epithelium.** (A) Cross-section of the intestine at E14.5. A subset of dividing cells (KI67, red) are associated with a T-shaped invagination of the apical surface (arrow). Other rounded mitotic cells are adjacent to a flat or V-shaped (asterisk) surface indentation. Apical surface is stained with antibodies to EZRIN (green). Clusters are also stained with antibodies to PDGFRα (red). Scale bar = 50 μm. (B, C) Confocal images of dividing cells (KI67 or pHH3, red) adjacent to a (B) V-shaped (asterisk) or (C) T-shaped (arrow) apical indentations (EZRIN, green). This T-shaped indentation is reminiscent of internalized cell rounding described in the *Drosophila* tracheal placode (Kondo and Hayashi, 2013). Scale bar = 5 μm.

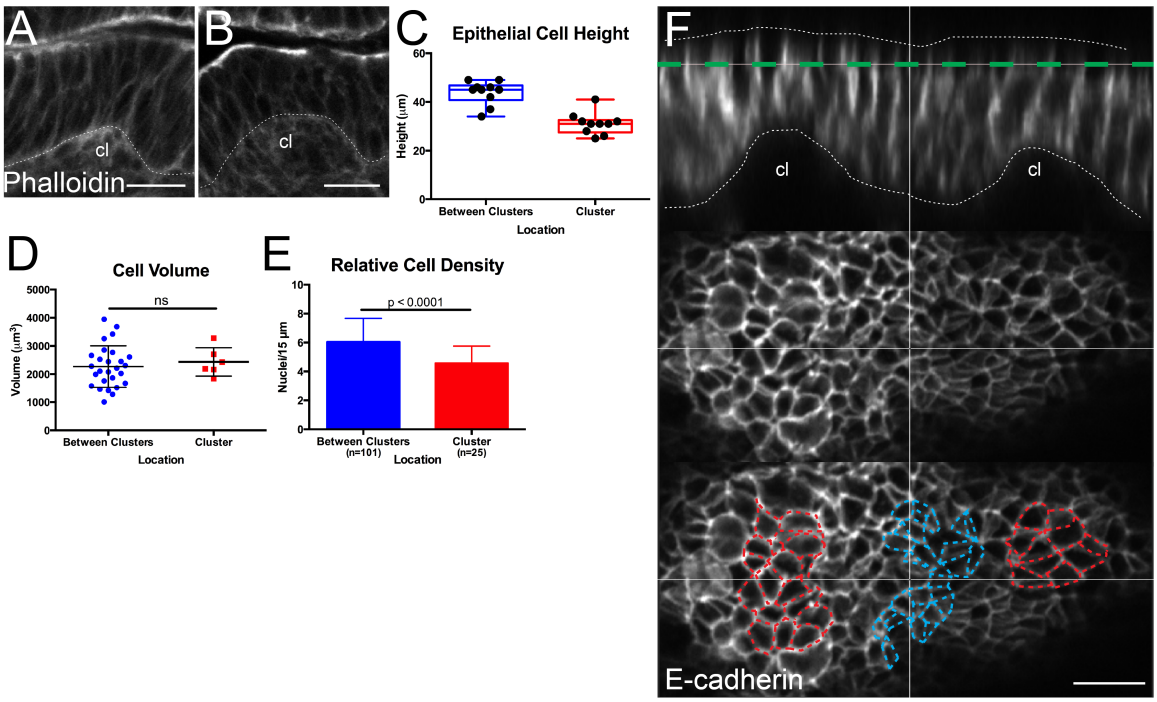


**Figure II-7. Epithelial cells above mesenchymal clusters are shorter and wider.** (A, B) Sections are stained with phalloidin (white). Mesenchymal clusters (cl) deform the overlying epithelium from the basal surface such that the epithelium is shorter over the cluster than adjacent to it (arrows). Scale bar = 20 μm. (C) Box and whisker plots comparing epithelial cell height over mesenchymal clusters and between clusters, showing the maximum, minimum, and median of the data sets. (D) Comparison of cell volume over and between clusters ($p > 0.05$, unpaired t test). Error bars represent standard deviation. (E) Quantification of epithelial nuclei per unit apical surface ("Relative Cell Density") above and between clusters ($p < 0.0001$, unpaired t test). Error bars represent standard deviation. (F) Cross-section through the epithelium (E-cadherin, white, and outlined) just after cluster formation. Bottom panels are projections of the plane highlighted in green. Note that cells over clusters (outlined in red) appear expanded circumferentially relative to cells between clusters (outlined in blue). Scale bar = 15 μm.

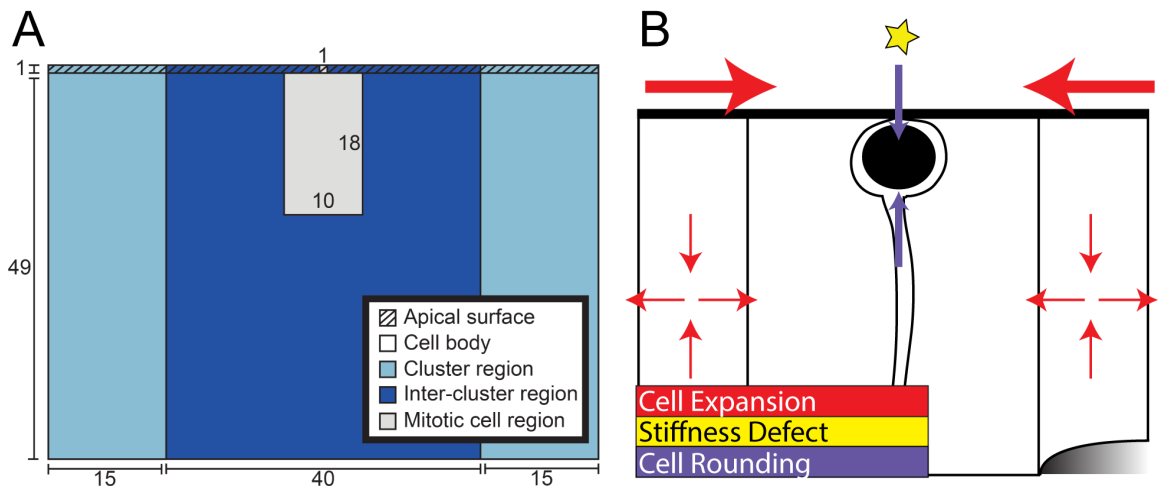


**Figure II-8. Geometry and variables used in the computational model.** (A) Schematic of the *in silico* representation of the early intestinal epithelium, with dimensions given in μm. (B) Three features of the physical forces within the epithelium were reconstituted in the model: cell expansion over clusters (red arrows), apical compliant defect at a mitotic cell (yellow star) and vertical contraction associated with mitotic cell rounding (purple arrows).

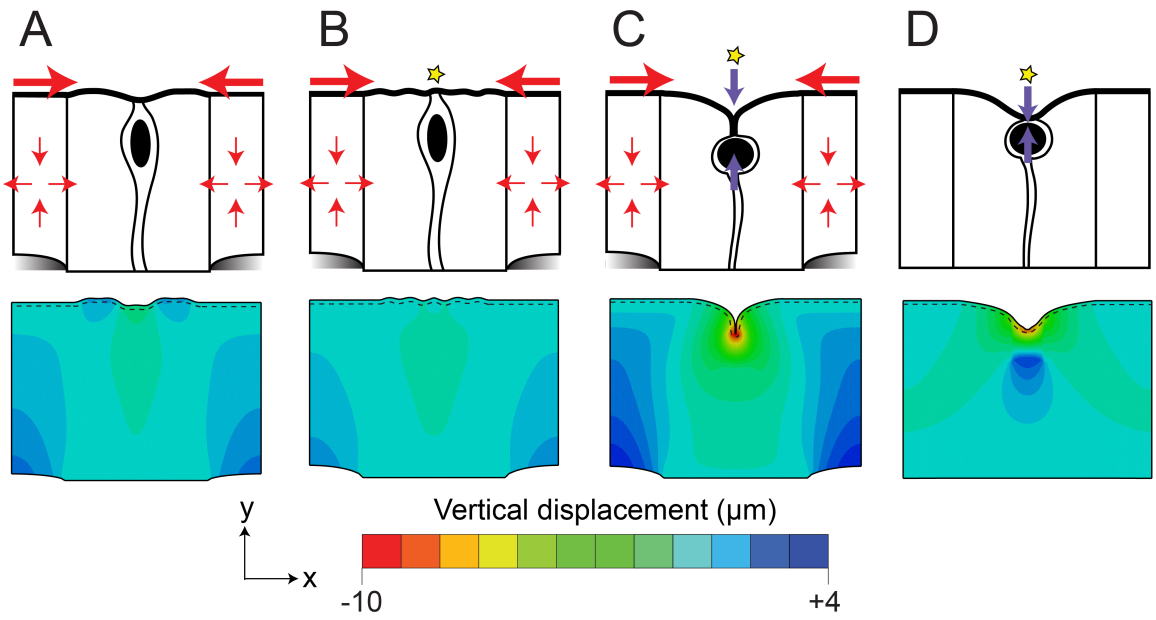


**Figure II-9. A computational model to investigate the forces involved in fold development.** (A-D) FEM plots from the simulations run in Abaqus, with apical surface emphasis added (dashed lines). The values of the vertical component of the displacement correspond to the colors on the heat map. Line drawings above summarize the results. (A, B) Compression from the clusters alone or in combination with a defect in stiffness to represent a mitotic cell is insufficient to cause an invagination. (C) Addition of a vertical contraction at a mitotic cell generates a fold with similar morphology to that observed *in vivo* (compare with Figure II-6, panel C). The combination of these three factors result in cell division-mediated invaginations in the intestinal epithelium. (D) Cell rounding in the absence of cell expansion results in a broader invagination that resembles V-shaped folds (compare with Figure II-6, panel B). Movies of these simulations are also provided (Movies 1-4, Supplemental).

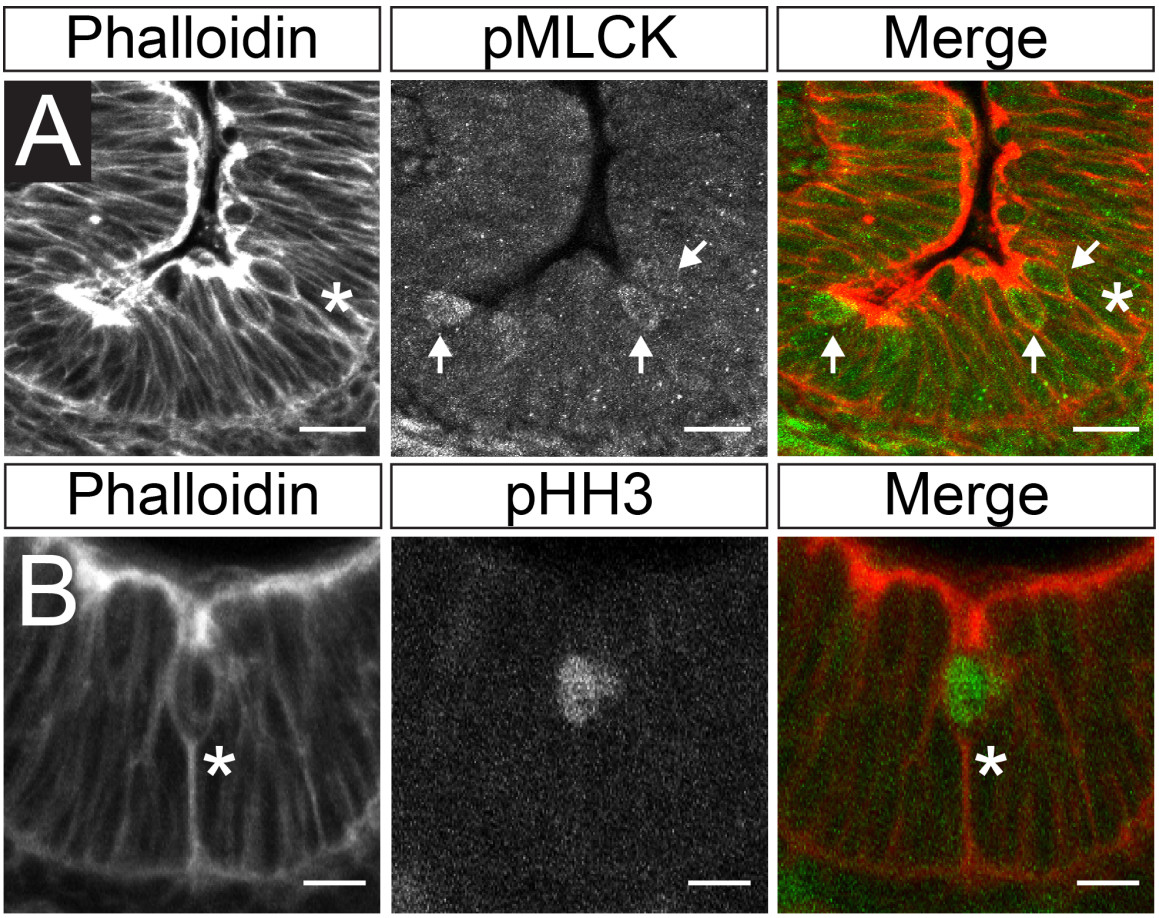


**Figure II-10. Mitotic cells at T-folds have basal processes enriched in actin.** (A) Staining with an antibody to pMLCK reveals increased expression in the cell bodies of rounded, dividing cells (arrows). Also note the tether of F-actin (stained with phalloidin, arrowhead) from the base of the cell body to the basal surface. Scale bar = 20 μm. (B) Dividing cell at an apical fold stained with an antibody against pHH3. A bright F-actin tether to the basal surface is visible. Scale bar = 10 μm.

| | Apical | | | Cell body | | |
|---|---|---|---|---|---|---|
| | Above cluster | Between clusters | Mitotic cell contact | Above cluster | Between clusters | Mitotic cell body |
| Young's modulus (kPa) | 10 | 10 | 2 | 0.5 | 0.5 | 0.5 |
| Poisson's ratio | 0.495 | 0.495 | 0.495 | 0.495 | 0.495 | 0.495 |
| C10 (kPa) | 1.67 | 1.67 | .336 | .0839 | .0839 | .0839 |
| D1 ($kPa^{-1}$) | 0.006 | 0.006 | 0.03 | 0.12 | 0.12 | 0.12 |
| Expansion ($^oC^{-1}$) | (0.5, 0) | (0, 0) | (0, -0.3) | (0.1, -0.1) | (0, 0) | (0, -0.3) |

**Table II-1. Mechanical properties assumed for the Holzapfel-Gasser-Ogden material model in Abaqus.** C10 and D1 are the moduli corresponding to the distortional and volumetric contributions to the strain energy function, respectively.

**Literature Cited**


**Brunser, O. and Luft, J. H.** (1970). Fine structure of the apex of absorptive cells from rat small intestine. *Journal of Ultrastructure Research* **31**, 291–311.

**Buckley, C. E., Ren, X., Ward, L. C., Girdler, G. C., Araya, C., Green, M. J., Clark, B. S., Link, B. A. and Clarke, J. D. W.** (2013). Mirror-symmetric microtubule assembly and cell interactions drive lumen formation in the zebrafish neural rod. *The EMBO Journal* **32**, 30–44.

**Burgess, D. R.** (1975). Morphogenesis of intestinal villi II. Mechanism of formation of previllous ridges. *Development* **34**, 723–740.

**Clarke, R.** (1967). On the constancy of the number of villi in the duodenum of the post-embryonic domestic fowl.

**Dekaney, C. M., Bazer, F. W. and Jaeger, L. A.** (1997). Mucosal morphogenesis and cytodifferentiation in fetal porcine small intestine. *The Anatomical Record* **249**, 517–523.

**Fehon, R. G., McClatchey, A. I. and Bretscher, A.** (2010). Organizing the cell cortex: the role of ERM proteins. 1–12.

**Forrester, J. M.** (1972). The number of villi in rat's jejunum and ileum: effect of normal growth, partial enterectomy, and tube feeding. *J. Anat.* **111**, 283–291.

**Garikipati, K.** (2009). The Kinematics of Biological Growth. *Applied Mechanics Reviews* **62**, 030801–030801–7.

**Gelbart, M. A., He, B., Martin, A. C., Thiberge, S. Y., Wieschaus, E. F. and Kaschube, M.** (2012). Volume conservation principle involved in cell lengthening and nucleus movement during tissue morphogenesis. *Proc. Natl. Acad. Sci. U.S.A.* **109**, 19298–19303.

**Goulet, O. and Ruemmele, F.** (2006). Causes and management of intestinal failure in children. *YGAST* **130**, S16–28.

**Goulet, O., Ruemmele, F., Lacaille, F. and Colomb, V.** (2004). Irreversible intestinal failure. *J. Pediatr. Gastroenterol. Nutr.* **38**, 250–269.

**Grosse, A. S., Pressprich, M. F., Curley, L. B., Hamilton, K. L., Margolis, B., Hildebrand, J. D. and Gumucio, D. L.** (2011). Cell dynamics in fetal intestinal epithelium: implications for intestinal growth and morphogenesis. *Development* **138**, 4423–4432.

**Helander, H. F. and Fändriks, L.** (2014). Surface area of the digestive tract – revisited. *Scandinavian Journal of Gastroenterology* **49**, 681–689.

**Helmrath, M. A., VanderKolk, W. E., Can, G., Erwin, C. R. and Warner, B. W.** (1996). Intestinal adaptation following massive small bowel resection in the mouse. *J. Am. Coll. Surg.* **183**, 441–449.

**Hughes, T. J.** (2012). *The finite element method: linear static and dynamic finite element analysis*. Courier Corporation.

**Karlsson, L., Lindahl, P., Heath, J. K. and Betsholtz, C.** (2000). Abnormal gastrointestinal development in PDGF-A and PDGFR-(alpha) deficient mice implicates a novel mesenchymal structure with putative instructive properties in villus morphogenesis. *Development* **127**, 3457–3466.

**Kolterud, A., Grosse, A. S., Zacharias, W. J., Walton, K. D., Kretovich, K. E., Madison, B. B., Waghray, M., Ferris, J. E., Hu, C., Merchant, J. L., et al.** (2009). Paracrine Hedgehog Signaling in Stomach and Intestine: New Roles for Hedgehog in Gastrointestinal Patterning. *Gastroenterology* **137**, 618–628.

**Kondo, T. and Hayashi, S.** (2013). Mitotic cell rounding accelerates epithelial invagination.

*Nature* **494**, 125–129.
**Lacroix, B., Kedinger, M., Simon-Assmann, P. and Haffen, K.** (1984). Early organogenesis of human small intestine: scanning electron microscopy and brush border enzymology. *Gut* **25**, 925–930.
**Li, B., Cao, Y. P., Feng, X. Q. and Gao, H.** (2011). Surface wrinkling of mucosa induced by volumetric growth: theory, simulation and experiment. *Journal of the Mechanics and Physics of Solids* **59**, 758–774.
**Lu, L., Oswald, S. J., Ngu, H. and Yin, F. C. P.** (2008). Mechanical Properties of Actin Stress Fibers in Living Cells. *Biophysical Journal* **95**, 6060–6071.
**Madara, J. L.** (2010). *Comprehensive Physiology*. (ed. Terjung, R. Hoboken, NJ, USA: John Wiley & Sons, Inc.
**Mathan, M., Moxey, P. C. and Trier, J. S.** (1976). Morphogenesis of fetal rat duodenal villi. *Am. J. Anat.* **146**, 73–92.
**Matsumoto, A., Hashimoto, K., Yoshioka, T. and Otani, H.** (2002). Occlusion and subsequent re-canalization in early duodenal development of human embryos: integrated organogenesis and histogenesis through a possible epithelial-mesenchymal interaction. *Anatomy and Embryology* **205**, 53–65.
**Matthews, H. K., Delabre, U., Rohn, J. L., Guck, J., Kunda, P. and Baum, B.** (2012). Changes in Ect2 Localization Couple Actomyosin-Dependent Cell Shape Changes to Mitotic Progression. *Developmental Cell* **23**, 371–383.
**Moeendarbary, E., Valon, L., Fritzsche, M., Harris, A. R., Moulding, D. A., Thrasher, A. J., Stride, E., Mahadevan, L. and Charras, G. T.** (2013). The cytoplasm of living cells behaves as a poroelastic material. *Nature Materials* **12**, 253–261.
**Monier, B., Gettings, M., Gay, G., Mangeat, T., Schott, S., Guarner, A. and Suzanne, M.** (2015). Apico-basal forces exerted by apoptotic cells drive epithelium folding. *Nature* **518**, 245–248.
**Moxey, P. C. and Trier, J. S.** (1979). Development of villus absorptive cells in the human fetal small intestine: A morphological and morphometric study. *The Anatomical Record* **195**, 463–482.
**Nakamura, K. and Komuro, T.** (1983). A three-dimensional study of the embryonic development and postnatal maturation of rat duodenal villi. *Journal of Electron Microscopy* **32**, 338–347.
**Nishimura, M., Inoue, Y. and Hayashi, S.** (2007). A wave of EGFR signaling determines cell alignment and intercalation in the Drosophila tracheal placode. *Development* **134**, 4273–4282.
**Odell, G. M., Oster, G., Alberch, P. and Burnside, B.** (1981). The mechanical basis of morphogenesis. *Developmental Biology* **85**, 446–462.
**Polyakov, O., He, B., Swan, M., Shaevitz, J. W., Kaschube, M. and Wieschaus, E.** (2014). Passive Mechanical Forces Control Cell-Shape Change during Drosophila Ventral Furrow Formation. *Biophysical Journal* **107**, 998–1010.
**Sauvanet, C., Wayt, J., Pelaseyed, T. and Bretscher, A.** (2015). Structure, Regulation, and Functional Diversity of Microvilli on the Apical Domain of Epithelial Cells. *Annu. Rev. Cell Dev. Biol.* **31**, 593–621.
**Schlüter, M. A., Pfarr, C. S., Pieczynski, J., Whiteman, E. L., Hurd, T. W., Fan, S., Liu, C.-J. and Margolis, B.** (2009). Trafficking of Crumbs3 during cytokinesis is crucial for lumen formation. *Molecular Biology of the Cell* **20**, 4652–4663.

**Shyer, A. E., Huycke, T. R., Lee, C., Mahadevan, L. and Tabin, C. J.** (2015). Bending Gradients: How the Intestinal Stem Cell Gets Its Home. *Cell* **161**, 569–580.

**Shyer, A. E., Tallinen, T., Nerurkar, N. L., Wei, Z., Gil, E. S., Kaplan, D. L., Tabin, C. J. and Mahadevan, L.** (2013). Villification: How the Gut Gets Its Villi. *Science* **342**, 212–218.

**Stelzner, M. and Chen, D. C.** (2006). To Make a New Intestinal Mucosa. *Rejuvenation Research* **9**, 20–25.

**Taniguchi, K., Shao, Y., Townshend, R. F., Tsai, Y.-H., DeLong, C. J., Lopez, S. A., Gayen, S., Freddo, A. M., Chue, D. J., Thomas, D. J., et al.** (2015). Lumen Formation Is an Intrinsic Property of Isolated Human Pluripotent Stem Cells. *Stem Cell Reports* **5**, 954–962.

**Tawk, M., Araya, C., Lyons, D. A., Reugels, A. M., Girdler, G. C., Bayley, P. R., Hyde, D. R., Tada, M. and Clarke, J. D. W.** (2007). A mirror-symmetric cell division that orchestrates neuroepithelial morphogenesis. *Nature* **446**, 797–800.

**Toyota, T., Yamamoto, M. and Kataoka, K.** (1989). Light and electron microscope study on developing intestinal mucosa in rat fetuses with special reference to the obliteration of the intestinal lumen. *Arch. Histol. Cytol.* **52**, 51–60.

**Walton, K. D. and Kolterud, A.** (2014). Mouse fetal whole intestine culture system for ex vivo manipulation of signaling pathways and three-dimensional live imaging of villus development. *J Vis Exp* e51817.

**Walton, K. D., Kolterud, A., Czerwinski, M. J., Bell, M. J., Prakash, A., Kushwaha, J., Grosse, A. S., Schnell, S. and Gumucio, D. L.** (2012). Hedgehog-responsive mesenchymal clusters direct patterning and emergence of intestinal villi. *Proc. Natl. Acad. Sci. U.S.A.* **109**, 15817–15822.

**Walton, K. D., Whidden, M., Kolterud, A., Shoffner, S. K., Czerwinski, M. J., Kushwaha, J., Parmar, N., Chandhrasekhar, D., Freddo, A. M., Schnell, S., et al.** (2016). Villification in the mouse: Bmp signals control intestinal villus patterning. *Development* **143**, 427–436.

**Wang, T., Yanger, K., Stanger, B. Z., Cassio, D. and Bi, E.** (2014). Cytokinesis defines a spatial landmark for hepatocyte polarization and apical lumen formation. *J. Cell. Sci.* **127**, 2483–2492.

**Yamaguchi, Y. and Miura, M.** (2012). How to form and close the brain: insight into the mechanism of cranial neural tube closure in mammals. *Cell. Mol. Life Sci.* **70**, 3171–3186.

**Yamaguchi, Y., Shinotsuka, N., Nonomura, K., Takemoto, K., Kuida, K., Yosida, H. and Miura, M.** (2011). Live imaging of apoptosis in a novel transgenic mouse highlights its role in neural tube closure. *The Journal of Cell Biology* **195**, 1047–1060.